Guidelines for Acquiring and Reporting Clinical Neurospectroscopy

Alexander Lin, PhD[1] Thao Tran, BS[2] Stefan Bluml, PhD[3] Sai Merugumala, BS[1] Hui-Jun Liao, BS[1] Brian D. Ross, MD, DPhil (Oxon)[1,2]

[1] Department of Radiology, Brigham and Women's Hospital, Boston, Massachusetts
[2] MRS Unit, Huntington Medical Research Institutes, Pasadena, California
[3] Department of Radiology, Children's Hospital Boston, Los Angeles California

Address for correspondence and reprint requests Alexander Lin, PhD, Department of Radiology, Brigham and Women's Hospital, 75 Francis Street, Boston, MA 02115 (e-mail: aplin@partners.org).

Semin Neurol 2012;32:432–453.

Abstract

Since the advent of CPT 76390 in 1998, magnetic resonance spectroscopy (MRS) of the brain, or neurospectroscopy, has moved from the realm of academic research into that of the clinical world. All major MR manufacturers have aided in the endeavor by automating neurospectroscopy so that it no longer requires an MR physicist and is a push-button technique that can be run by technologists just as a typical MR sequence. Thousands of studies have demonstrated the clinical efficacy of neurospectroscopy, and there are many medical reviews of how this technique can be applied across a wide range of neurologic disorders. However, few studies address the practical issue of acquiring and reporting neurospectroscopy in a clinical practice. Based on clinical experience at three different sites across the country and nearly two decades of applications training for technologists and radiologists at international clinical neurospectroscopy courses, the guidelines described in this article demonstrate proven protocols for clinical diagnosis and outline the strategies involved in acquiring, interpreting, and reporting clinical neurospectroscopy successfully. A standard operating procedure used across the three sites is described and high reproducibility across different platforms is shown.

Keywords
- magnetic resonance spectroscopy
- clinical efficacy
- standardization
- neurologic disease
- reproducibility

Magnetic resonance spectroscopy (MRS) of the brain, neurospectroscopy, is a noninvasive and quantitative method of measuring chemical concentrations of metabolites in vivo. As such, it has been employed in research and in the clinic for well over three decades and proven to be diagnostically significant across a broad range of neurologic diseases (►**Table 1**). Over 28,000 publications were identified in a study in 2006[1] that described the use of MRS in clinical diagnosis where a majority of the studies demonstrated technical feasibility of MRS as well as contributions to diagnosis and better understanding of the underlying pathophysiology. Similarly, there are hundreds of reviews on the use of MRS in different neurologic diseases[2–71] and we have cited several recent reviews for each of the clinical indications listed in ►**Table 1**, thereby demonstrating the clinical utility of MRS. MRS is also widely accessible. Commercial MRS acquisition and postprocessing software approved by the Food and Drug Administration (FDA) exists across all major MR platforms and field strengths greater than 1.5 Tesla (T). In addition to being FDA-approved, MRS also has a Category 1 CPT code (76390) and is actively reimbursed (see the subsection, Reimbursement).

Aims

Despite evidence of its technical feasibility, diagnostic importance, wide availability, and reimbursement, there has not been widespread application of MRS as a routine clinical tool

Issue Theme Diagnostic Neuroimaging; Guest Editor, Joshua P. Klein, MD, PhD

DOI http://dx.doi.org/10.1055/s-0032-1331814.
ISSN 0271-8235.

Table 1 Clinical Indications for Magnetic Resonance Spectroscopy

1. Evidence or suspicion of primary or secondary neoplasm (pretreatment and posttreatment)[8–12]
2. Grading of primary glial neoplasm, particularly high-grade versus low-grade glioma[13–15]
3. Evidence or suspicion of brain infection, especially cerebral abscess (pretreatment and posttreatment) and human immunodeficiency- (HIV-) related infections[16–18]
4. Seizures, especially temporal lobe epilepsy[19,20]
5. Evidence or suspicion of neurodegenerative disease, especially Alzheimer's disease, Parkinson's disease, and Huntington's disease[21–23]
6. Evidence or suspicion of subclinical or clinical hepatic encephalopathy[24,25]
7. Evidence or suspicion of an inherited metabolic disorder such as Canavan's disease and other leukodystrophies[26–29]
8. Suspicion of acute brain ischemia or infarction[30–32]
9. Evidence or suspicion of a demyelination or dysmyelination disorder[33–35]
10. Evidence or suspicion of traumatic brain injury[36–40]
11. Evidence or suspicion of brain developmental abnormality and cerebral palsy[41–43]
12. Evidence or suspicion of other neurodegenerative diseases such as amyotrophic lateral sclerosis[44,45]
13. Evidence or suspicion of chronic pain syndromes[46,47]
14. Evidence or suspicion of chromosomal and inherited neurocutaneous disorders such as neurofibromatosis and tuberous sclerosis[48–50]
15. Evidence or suspicion of neurotoxicity disorders[51–53]
16. Evidence or suspicion of hypoxic brain injury[54–56]
17. Evidence or suspicion of spinal cord disorders such as tumors, demyelination, infection, and trauma[57,58]
18. Evidence of neuropsychiatric disorders such as depression, posttraumatic stress syndrome, and schizophrenia[59–62]
19. Differentiation between recurrent tumor and treatment-related changes or radiation injury[63–65]
20. Differentiation of cystic lesions, e.g., abscess versus cystic metastasis or cystic primary neoplasm[66]
21. Evidence or suspicion of cerebral vasculitis, systemic lupus erythematosus (SLE), and neuropsychiatric systemic lupus erythematosus (NPSLE)[67,68]
22. Evaluation of response to treatment of neurologic disorders[69–71]
Adapted from American College of Radiology and the American Society of Neuroradiology Practice Guideline for the Performance and Interpretation of Magnetic Resonance Spectroscopy of the Central Nervous System.[74] Focal diseases in **bold**, global diseases in *italics*. Those diseases that can utilize both paradigms are both ***bold and italics***, such as demyelinating disorders that can be focal (multiple sclerosis plaques) or global (assessing normal-appearing white matter). Selected reviews are cited with each indication.

in diagnosis and monitoring of neurologic disorders. In the early stages of MRS development, spectral acquisition required multiple steps and manual changes, often requiring the input of an MR physicist, which limited MRS to sites with specific expertise. Although MR manufacturers have now developed relatively automated methods of MRS data acquisition that removes this limitation,[72,73] questions of protocoling and issues such as voxel placement remain unfamiliar to MR technologists. Similarly, radiologists who are oriented toward anatomy as opposed to biochemistry, and therefore unfamiliar with interpretation and reporting of MRS, may have also hindered more widespread adoption.[6]

Therefore, the goal of this review is to demystify MRS methodologies by providing simple guidelines that facilitate the use of MRS in the clinical environment covering both data interpretation and reporting. These guidelines were developed over the course of nearly two decades of clinical neurospectroscopy courses that we have organized and taught both locally and internationally, as well as our own personal experience acquiring clinical neurospectroscopy at three different sites. Although it is impossible to provide the level of detail given on a 3-day course, a general approach will be described. Rather than focusing on specifics for each disease, a more practical guide to data acquisition, interpretation, and reporting will be given. However, for the benefit of the reader, we have also provided a comprehensive list of reviews that cover the major clinical applications of MRS: The cited references in ►**Table 1** are intended to provide more in-depth detail for the reader for MRS in specific diseases. We also recommend—and intend to compliment with this practical review—a previous review published in *Seminars in Neurology*[4] which covers the clinical applications of MRS.

Evidence-based medicine (EBM) studies have argued that MRS is too variable to be used reproducibly at multiple sites due to between-manufacturer scanner differences, differences in data collection and analysis methods, and other technical problems.[1] Indeed, the lack of consistent procedures among sites for MRS spectra acquisition and analyses has made it difficult to interpret and compare results across investigations. The variance issue, in turn, has inhibited

widespread use of clinical MRS by physicians, research investigators, and clinical trial experts. As an initial step in addressing this gap in clinical use, we provide evidence that the standard MRS protocols described in this article can be used for performing MRS at different sites and provide comparable results. The goal is to demonstrate a standardized MRS procedure suited to cross-platform and multisite applications to support future clinical studies in CNS disorders.

Finally, we conclude with the current status of reimbursement and future directions. Here we will provide evidence of reimbursement for MRS as well as strategies for successful billing. As progress is made toward better integration of MRS into clinical practice, we will examine future directions of clinical spectroscopy by describing the types of studies that must be conducted to reverse EBM study results and move MRS out of "investigational" status to its rightful place as an important diagnostic tool.

The Virtual Biopsy: Global versus Focal Spectroscopy

Often described as a "virtual biopsy," MRS obtains chemical signals, or metabolites, from a region of interest (ROI or voxel) whereby each metabolite is reflective of brain metabolism and physiology as shown in ►**Fig. 1** (full details of the metabolites and their roles in disease diagnosis are described in the subsection, Metabolites and Their Roles in Disease Diagnosis). As with true biopsies, the diagnostic accuracy of the MRS virtual biopsy is based on how and where the MRS is acquired. The location of the biopsy is dependent on the disease. We have therefore developed two paradigms, or overall frameworks, for acquiring and analyzing MRS data that are based on the clinical indication that we describe as "focal" or "global." These paradigms translate into different protocols, each of which will require a different approach to the parameters described in a later section as well as interpreting and reporting the results. The definitions of global and focal spectroscopy follow.

Global Spectroscopy

In global spectroscopy, spectra are acquired from a specific region of interest that is the same in all patients. For example, in diagnosing Alzheimer's disease, the technologist will place the voxel in the gray matter in the posterior parietal lobe of the brain. In this paradigm, very little changes from patient to patient. A well-defined protocol is used for this type of spectroscopy. This not only simplifies data acquisition, but analysis and reporting of the MRS results are straightforward as well. Results from each exam are compared against a normative database and reported based on differences to those values, similar to a blood test. However, the validity of the comparison to the normative database is contingent upon the consistency of the data acquisition methods; therefore, attention to protocol details is critical.

Focal Spectroscopy

In focal spectroscopy, spectra are acquired from specific regions of interest that are variable from patient to patient. For example, in brain tumor spectroscopy, the location, size, and homogeneity of the tumor will differ from patient to

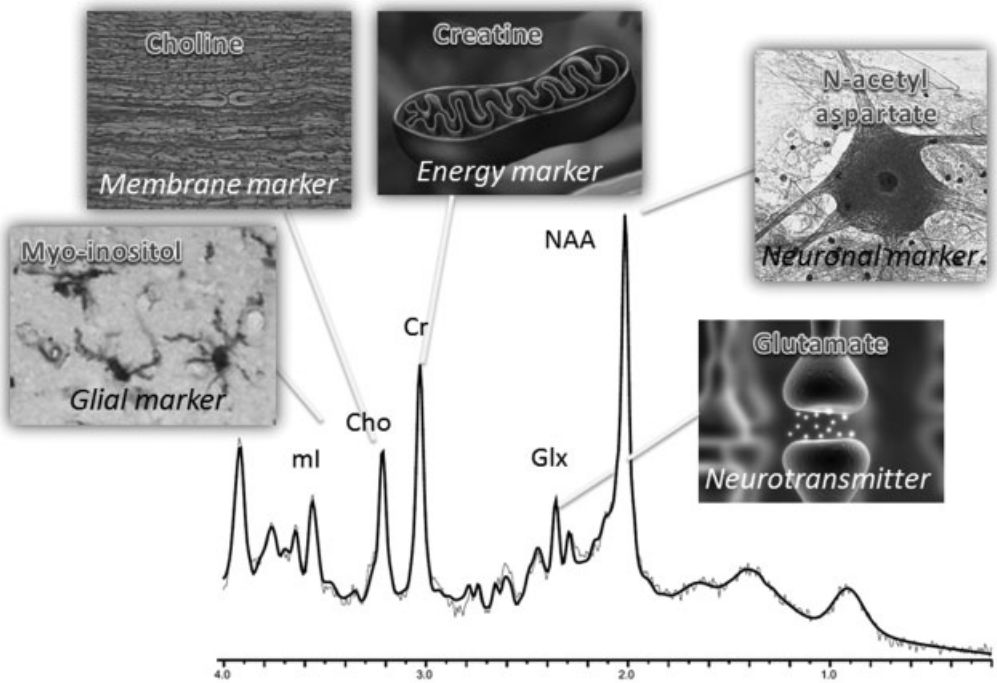

Fig. 1 The virtual biopsy. Magnetic resonance spectroscopy is a direct measure of the metabolites that provides a window into the underlying pathophysiology represented by the images. N-acetylaspartate (NAA), the tallest peak in the spectrum, is proportional to the number of functioning neurons. Glutamate/glutamine (Glx) is a neurotransmitter. Creatine (Cr) is an energy marker related to mitochondrial function. Choline (Cho) is a membrane marker. Myoinositol (mI) is a glial marker.

patient. It is therefore critical to understand the underlying concepts behind each parameter such that they are used to maximize technical advantages in different situations. Input from the radiologist and referring physician is valuable for determining voxel location and size that will be used for data acquisition. However, those physicians must be aware of the guidelines and limitations of voxel placement and size as described below.

Although there may be subtle differences in protocols for specific clinical indications, the two types of protocols can be generalized into global and focal diseases. ►**Table 1** lists the clinical indications for MRS described by the American College of Radiology (ACR) and the American Society of Neuroradiology (ASNR)[74] with the global and focal diseases highlighted. In some indications, a global or focal approach can be used. For example, multiple sclerosis could be focal (multiple sclerosis plaques) or global (assessment of normal-appearing white matter) depending on physician request. Therefore, depending on the clinical indication, either the global or focal method will be utilized in the data acquisition section that follows.

Data Acquisition

Voxel Position

Single Voxel versus Chemical Shift Imaging

Single-voxel spectroscopy (SVS) is acquired using three slice-selective radiofrequency pulses where the intersection of the pulses defines the region of interest (ROI) or voxel resulting in a single spectrum for interpretation and analysis within several minutes. This method is ideally suited for global spectroscopy given that specific regions of the brain can be selected and examined for diagnosis. However, in focal disease, where the extent of a lesion can provide valuable clinical information, obtaining spectra in many different areas of the lesion would be time consuming. Multivoxel spectroscopy, also called chemical shift imaging (CSI) overcomes this issue by adding an additional phase-encoding step that allows for spatial encoding of a larger volume such that it is divided into smaller voxels which can be summed, or select chemical shifts can be color-coded into chemical shift maps as shown in ►**Fig. 2**. This method can be extended into the third dimension to provide almost complete coverage of the brain.

Although it is tempting to replace SVS with CSI, thereby eliminating the need for careful voxel placement, there are several drawbacks to CSI such that SVS is still critical for accurate diagnosis in clinical spectroscopy. Diagnosis is often made in comparison with a normative database. To date, a normative database for CSI does not exist. Furthermore, CSI is not as reproducible as SVS[75]; therefore, it is less sensitive to the more subtle changes that are necessary for diagnosis in global diseases. In focal disease, such as brain tumors, where choline changes are increased by 100–200% of normal, such sensitivity is not required; however, in diseases such as Alzheimer's disease where changes in NAA and myoinositol on the order of 15% may be diagnostic, the coefficient of variation (CV) of CSI is not sufficient.

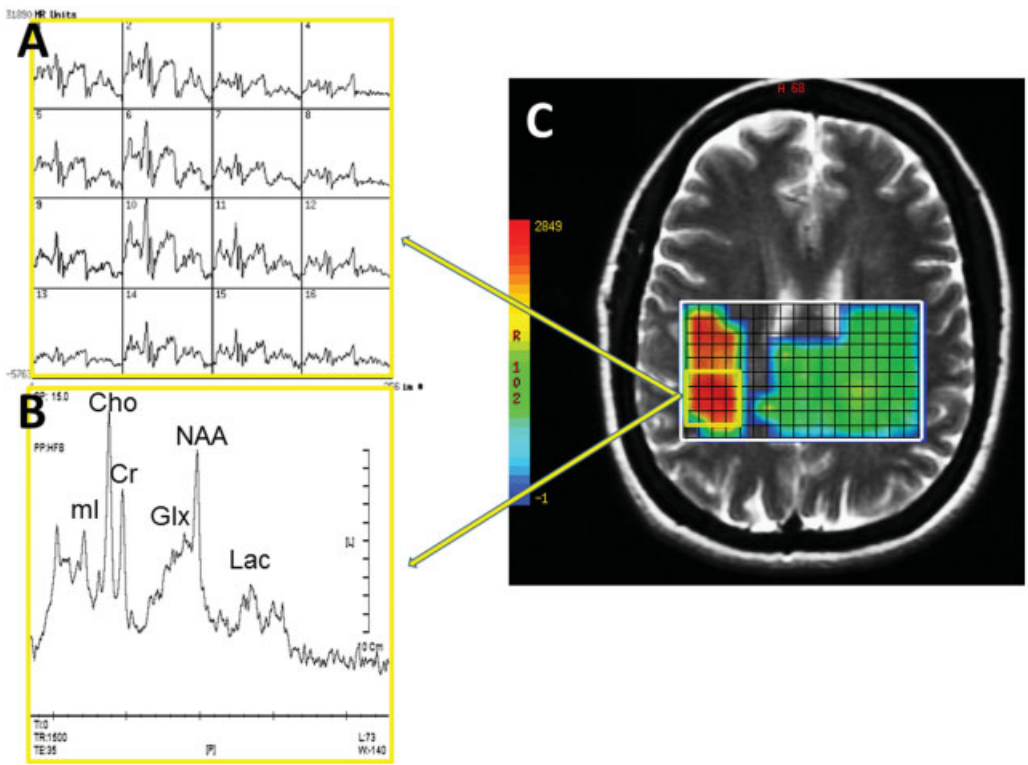

Fig. 2 Chemical shift imaging. (**A**) Spectral grid of individual spectra obtained from the yellow region of interest. (**B**) Single voxel spectrum acquired from the same region confirms the CSI results of increased choline in that region as well as evidence of lactate (Lac) and reduced NAA. (**C**) Color-coded metabolite map of Choline (Cho) corrected by creatine (Cr) where red shows high Cho/Cr amplitude and blue is low.

Table 2 Clinical Protocol Decision Matrix

Diagnosis	Protocol
1. Dementia, memory loss	1. Posterior GM/Parietal WM
a. Frontal lobe Lewy Body dementia	a. + Frontal GM
2. Focal lesion (tumor, recurrence)	2. Focal SV-MRS, CSI
a. + Contrast	a. + T1w, T1w + c, MRS OK after Gad
b. Versus stroke	b. + DWI, voxel in center of lesion and rim
c. versus abscess	c. voxel in the center of lesion, maximize PV
d. Radiation necrosis versus recurrence	d. Voxel at the edge of the lesion
3. Demyelinating disease, white matter disease	3. Parietal WM
a. Multiple sclerosis (MS) w/o lesions	a. Parietal WM
b. Multiple sclerosis (MS) w/ lesions	b. If lesion > 3 cc, use SVS. If < 3 cc, use CSI.
4. Epilepsy	4. Posterior GM/Parietal WM
a. Mesial temporal lobe epilepsy	a. + L/R Temporal lobe
b. Known focus	b. Focal SV (bilateral)
5. Parkinson/Huntington disease	5. Posterior GM/parietal WM, Left and/or right basal ganglia
6. Hepatic encephalopathy (HE)	6. Posterior GM/parietal WM (earliest changes in WM)
7. Global hypoxia	7. Posterior GM/parietal WM
8. Trauma	8. SV-MRS away from blood/lesions
a. Possible hypoxia	a. Posterior GM
b. No hypoxia	b. Parietal WM
9. Systemic diseases, unknown not focal	9. Posterior GM/Parietal WM

Abbreviations: GM, gray matter; WM, white matter; MRS, magnetic resonance spectroscopy; CSI, chemical shift imaging; SVS, single-voxel spectroscopy; SV, single voxel; Gad, gadolinium; T1w, T1-weighted; T1w + c, T1-weighted with contrast; DWI, diffusion weighted imaging.

Finally, on modern clinical scanners the majority of CSI acquisitions are set up for long-echo MRS, which also eliminates important diagnostic metabolites (such as myo-inositol). Therefore, in the clinic, SVS is still an important diagnostic tool that should be used in conjunction with CSI in focal diseases and used almost solely for global diseases as described in ►**Table 2**. We describe below how to place voxels for SVS for this purpose.

Global Spectroscopy

The advantage of global spectroscopy is that the protocol is straightforward: A set voxel location is predetermined and acquired. The key to voxel placement is to use anatomic landmarks to ensure greatest reproducibility of results. We begin with our gray matter (GM) protocol. A single voxel is placed in the posterior cingulate gyrus as shown in ►**Fig. 3**. The voxel is positioned such that it is in the center of the gray matter of the cingulate gyrus as shown in the axial plane. Special care is taken to avoid the white matter in the corpus callosum. The coronal plane is used to ensure that the voxel is placed medially, covering both the left and right posterior gyri. Voxel placement in the sagittal plane should ensure that the voxel is not too close to the skull which can often be the case in older subjects or patients with dilated ventricles. This region of the brain has been shown to be diagnostic across several diseases including Alzheimer's disease and other dementias,[21,22] traumatic brain injury,[36,76] Parkinson's disease,[77] metabolic disorders,[78] mitochondrial disorders,[28] schizophrenia,[79] hepatic encephalopathy,[25] and many other diseases.[71] The reason this region is sensitive to this broad range of diseases is because it is one of the most homogeneous parts of the brain, providing excellent quality spectra with high signal-to-noise ratio (SNR) and linewidths. This in turn improves the diagnostic accuracy of spectra acquired from this brain region. ►**Table 2** describes some situations in which this protocol is used.

Other brain regions that have been utilized for global spectroscopy include parietal white matter (WM), often used to assess changes in myelination and other white matter disorders; as well as anterior gray matter and white matter for assessing frontal lobe changes. The voxel locations are shown in ►**Fig. 4**. Although the hippocampus may appear to be an obvious choice for diseases such as Alzheimer's disease where pathophysiologic and morphologic changes may manifest, this region suffers from susceptibility artifacts that reduce spectral quality and reproducibility.[80] As a result, the CV values range from 15 to 44% as opposed to the posterior cingulate voxel where CV values range from 2 to 3%, therefore allowing subtle changes in brain chemistry, such as a 10% change in NAA to be readily detected in the posterior

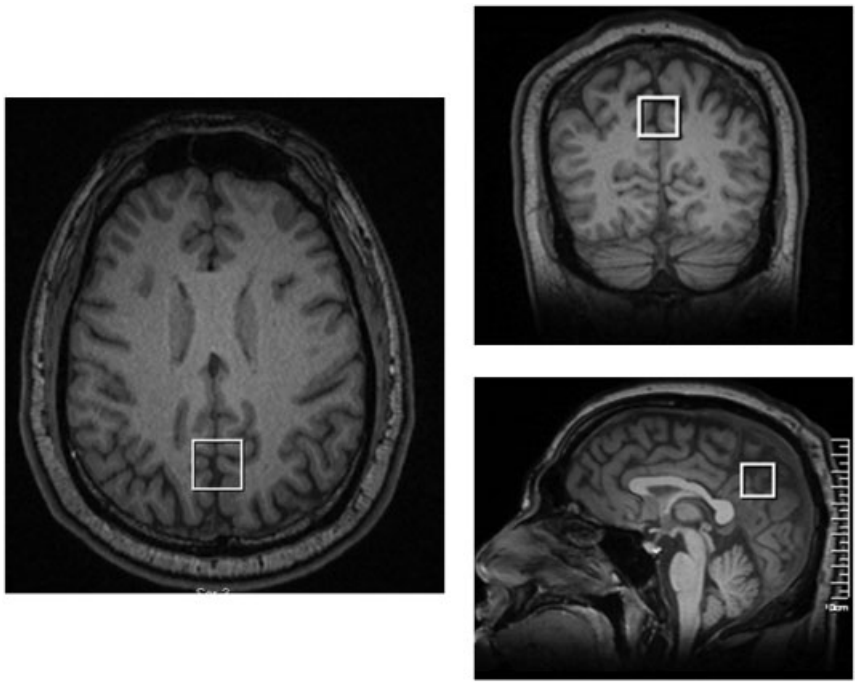

Fig. 3 Posterior gray matter (GM) voxel position in the axial (**A**), coronal (**B**), and sagittal (**C**) planes of three-dimensional magnetization prepared rapid gradient echo magnetic resonance imaging (3D MPRAGE MRI).

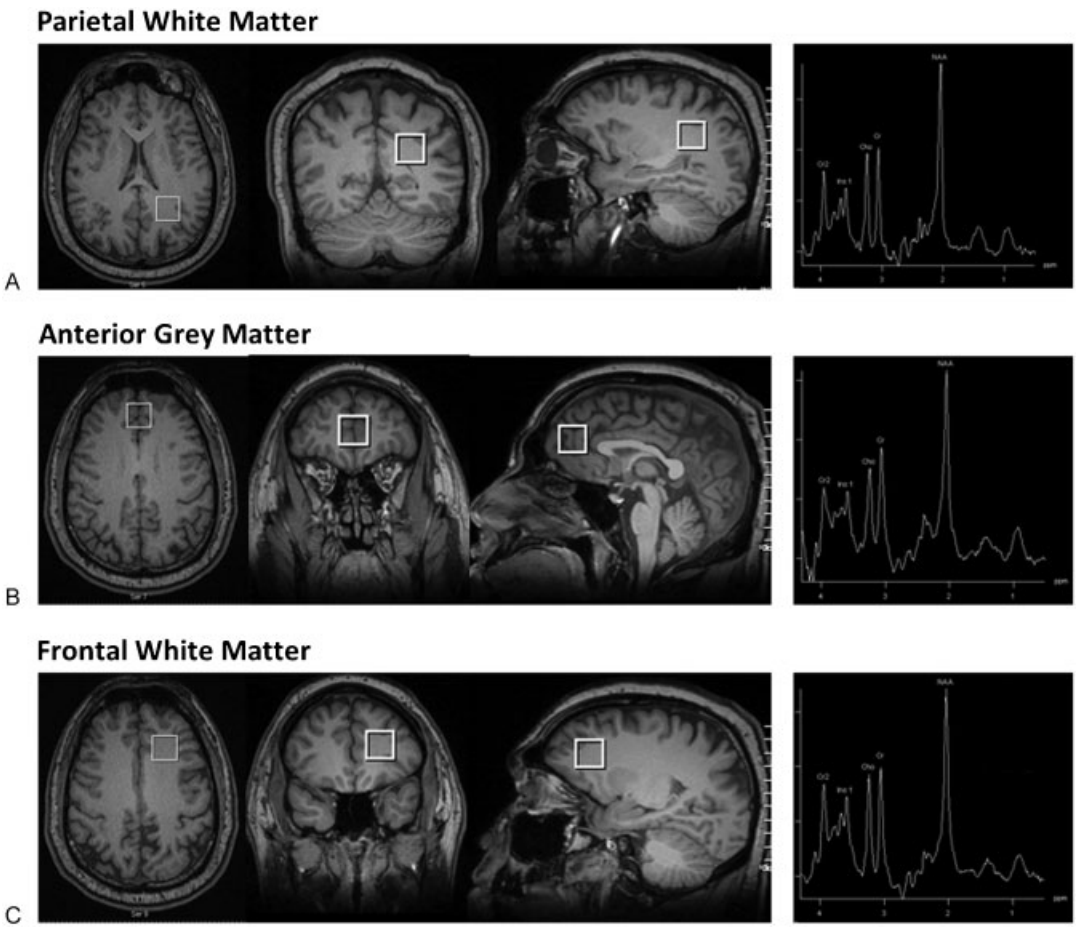

Fig. 4 Additional global voxel positions. Parietal white matter (**A**), anterior gray matter (**B**), anterior white matter (**C**) voxel positions shown in the axial, coronal, and sagittal planes of three-dimensional magnetization prepared rapid gradient echo magnetic resonance imaging (3D MPRAGE MRI), with representative spectra from each region (right).

cingulate but not the temporal lobes. Likewise, other regions of the brain where spectroscopy is not as reproducible are less ideal for clinical neurospectroscopy.

Focal Spectroscopy

The concern for reproducibility and susceptibility artifacts are especially prominent for focal spectroscopy. Unlike global spectroscopy, the location of the lesions in focal spectroscopy will not be the same from patient to patient. In this case, it is more important to optimize the position such to increase partial volume of the lesion, homogeneity, and of course, signal. Although in each pathology, different techniques in determining voxel position can be used, there are some areas of the brain or pathology as discussed below that should be avoided.

Skull

Stay away from the surfaces of the brain. The lipids that lie in the meninges of the brain, within the bones of the skull, or in the scalp can contaminate spectra in two ways: (1) By creating an overriding lipid signal that can dominate the entire spectrum as shown in ►**Figs. 5a, b** and **6a**. (2) An artifact that can result is "an out of volume lipid artifact," which results in inverted peaks in the 1.2 to 2.0 range that can affect NAA measures as shown in ►**Fig. 6b**. By carefully checking all three planes when placing the voxel, this error can be avoided.

Necrosis

As described above, lipids can cause severe problems with spectra. As the necrotic center of a tumor contains lipid, the strategy is to move away from the necrosis to the edge of the lesion. Although there is some loss of partial volume of the lesion, the resulting spectrum is readable and interpretable.

Blood

Blood contains heme-iron, which is paramagnetic and will destroy signal coming from brain tissue. Postsurgical locations or highly necrotic centers can pool blood that leads to poor shim (►**Fig. 6c**) and/or artifacts (►**Fig. 6d**) in the spectrum.

Open Space

Areas of open space such as in air sinuses adjacent to the temporal lobes should be avoided as they will also result in susceptibility artifacts as seen in ►**Fig. 6c**. Similarly, areas of resection should also be avoided.

Cerebrospinal Fluid (CSF)

Contrary to popular belief, partial volume of CSF from the ventricles or atrophy is not a major problem. Although the tissue–CSF interface may cause some susceptibility, it is very minor compared with the artifacts that result from the aforementioned regions. Because the majority of the

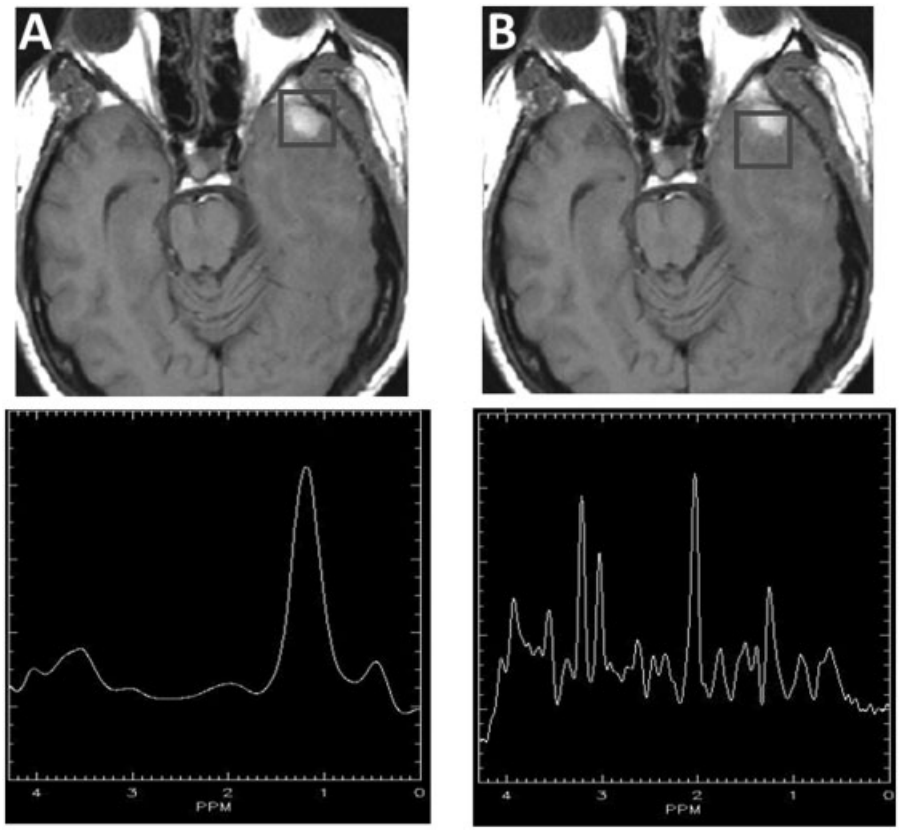

Fig. 5 Example of poor voxel placement. (**A**) Incorrect voxel placement on the image (top) results in lipid contamination in the magnetic resonance spectrum (bottom). (**B**) Correct voxel placement with partial volume of lesion as shown on the image (top), but avoiding lipid contamination and resulting in a diagnostic spectrum (bottom).

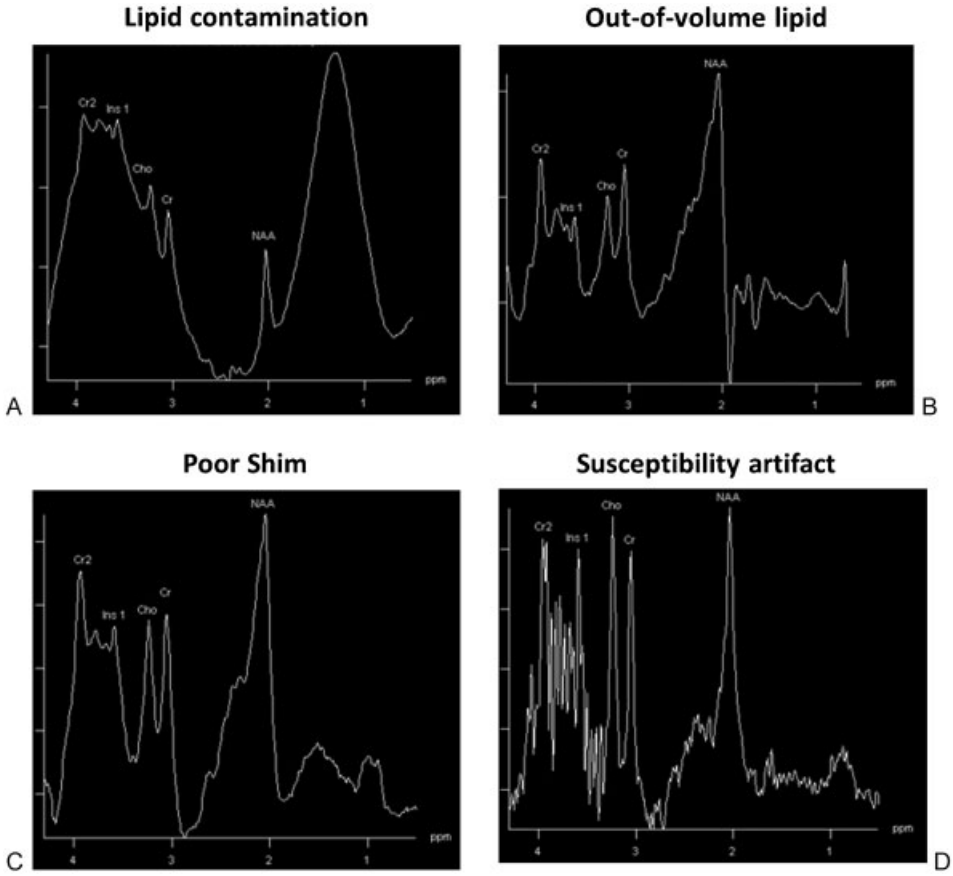

Fig. 6 Gallery of artifacts. Representative spectra of different artifacts that can arise in magnetic resonance spectroscopy. (**A)** Lipid contamination resulting from patient head movement. (**B)** Out-of-volume lipid artifact results in an inverted peak upfield of 2 ppm, which makes it difficult to assess the N-acetylaspartate peak (NAA). (**C)** Poor shimming results in broad linewidths causing choline (Cho) and creatine (Cr) peaks to overlap and indistinctness of the glutamate/glutamine (Glx) region. (**D)** Susceptibility artifact results in the artifacts between 3.2 and 4 ppm making it impossible to characterize the myoinositol (mI) region.

voxel should not be placed in CSF as it will result in SNR loss (CSF contains no metabolites), it is better to include partial volume of the CSF rather than getting too close to the skull.

Dr. Roland Kreis has written an excellent guide[81] to the additional artifacts that plague spectroscopy, which includes more examples of artifacts and explanations.

Partial volume is one of the attributes of focal spectroscopy that can be optimized with voxel position. Studies have shown that it is better to obtain spectra from the edge of the lesion away from the brain. Obtaining spectra from the edge may not have complete partial volume, but it does guarantee an interpretable spectra. ►**Figure 7** demonstrates how the metabolite concentrations change with partial volume. Six different voxels were acquired in a single subject and the resulting metabolite ratios were calculated with each partial volume. At 100% partial volume, where the lesion is fully contained within the voxel, choline is high and NAA is reduced, as expected. However, even at 25% partial volume, the Cho/Cr ratio is 1.5, which is higher than normal, and NAA is 1.0, which is also lower than normal. Therefore, a diagnosis can still be made by assuming linearity of the metabolite levels with partial volume.

Contralateral Voxel

A second spectrum can be obtained that is contralateral to the focal voxel to provide a comparable "normal" spectrum with which to compare the pathologic one. The danger of trusting such a spectra is that in some pathologies, the changes in metabolism are not limited to the region of interest such as in glioblastoma.[82] Studies have also shown that radiation therapy causes global changes to the brain[83,84] which affect the metabolite ratios of "normal" spectra. As the radiologist becomes more familiar with the spectral patterns in different areas of the brain, it will not be necessary to provide a so-called normal contralateral spectrum.

Contrast Agent

A frequently asked question is whether MRS should be acquired before or after contrast is given. Obviously, the chief advantage of postcontrast MRS would be to target the region of greatest enhancement; however, earlier studies reported that contrast agents could reduce the choline signal and therefore affect MRS accuracy.[85,86] Fortunately, multiple studies have now examined this issue and have concluded that while contrast agents may have a small effect on choline signal, it is not enough to alter the diagnostic quality of the MRS studies.[87–91]

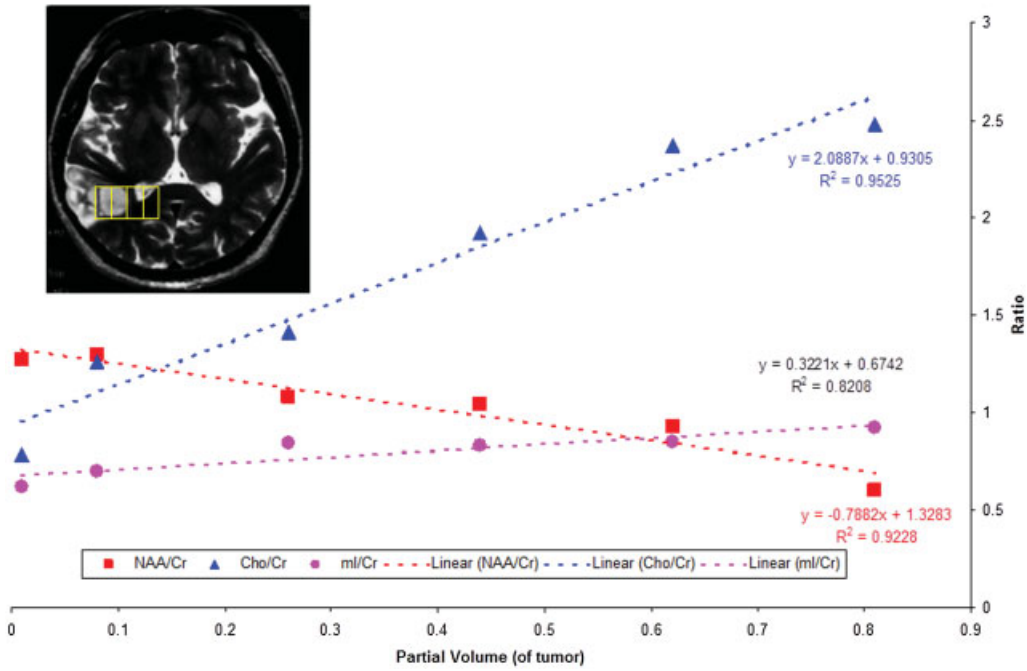

Fig. 7 Partial volume study of voxel position. A well-circumscribed lesion (inset) offered the opportunity to determine the relationship between partial volume and metabolite peak heights of N-acetylaspartate/ creatine (NAA/Cr; red), choline/creatine (Cho/Cr; blue), and myoinositol/ creatine (mI/Cr; purple). The results show that the partial volume varies linearly as evidenced by the high r^2 values of the linear regression (dotted lines).

Signal-to-Noise Ratio

Voxel Size

Signal-to-noise ratio (SNR) is highly dependent on voxel size. A typical MRS voxel size is 2.0 × 2.0 × 2.0 cm^3 (8 cc). This is an optimal voxel size for most applications except notably in neonatal neurospectroscopy, where smaller voxel size may be required. In global diseases, voxel sizes are well established and should not change from patient to patient. In some protocols, the default of 8 cc may not be used due to location-specific optimization; however, all patients examined with that particular protocol must have the same voxel size.

With focal neurospectroscopy, 8 cc may not be suitable to obtain enough partial volume of the lesion or may be too small for a large lesion. For lesions that are smaller than 8 cc, it is best to obtain a spectrum from the larger volume. A common mistake is to shrink the voxel to too small a volume. In that case, there will not be enough signal to generate a readable spectrum. If the first voxel is successful, then one can shrink the voxel to increase the partial volume. This can be diagnostically useful in that the increase in partial volume of tumor should result in increased Cho. If this change is not observed, the lesion in question may not be neoplastic.

Similarly, one should not increase voxel size to accommodate larger lesions. The larger the voxel, the greater the chances of observing inhomogeneity effects (such as artifacts and eddy current problems) in the volume. It is best to use a volume between 8 to 27 cc and to change voxel position instead of trying a larger voxel. As discussed earlier, placing the voxel at the edge of the lesion is the optimal approach.

Number of Averages

Directly related to voxel size is the number of averages. In the global paradigm where you already have a defined size and location, the number of averages is the same for every acquisition as it does not need to be adjusted for signal and homogeneity effects. The data from the defined size and location should also always be acquired with the same number of averages.

In the focal paradigm, adjustments are dependent on the size of the voxel. Generally, an 8-cc voxel requires 128 averages for a high-quality spectrum. SNR is proportional to the square root of the number of averages. Therefore, if the voxel volume is reduced by half, the number of averages must be increased by 4 times to 512 averages to maintain the same SNR. Therefore, if you use a very small volume such as 2 cc, you would require 2,048 averages, which at a repetition time of 2 seconds would take 68 minutes! This implies that shrinking the voxel size is a practice that should be avoided when possible.

Pulse Sequence

Repetition Time and Echo Time

Typical repetition times (TR) for clinical neurospectroscopy are 1500 ms for 1.5T and 2000 ms for 3.0T. Although fully relaxed spectra using TR of 5000 mms are ideal and provide greater SNR, the tradeoff in scan time is suboptimal for clinical scans. Echo time (TE) on the other hand is a somewhat more controversial topic. Historically, the arguments for using intermediate (135–144 ms) and long (244–288 ms) TE is that they provide better baselines, remove unwanted

lipid signal, and lactate inversion, allowing for easier detection. However, longer TE also results in signal loss both in SNR and the metabolites that can be detected. Metabolites with short T2 time such as myoinositol, glutamate, glutamine, taurine, scylloinositol, etc., can be observed at short TE of 21 to 35 ms. These metabolites are critical to the diagnostic power of neurospectroscopy. For example, the diagnosis of Alzheimer's disease is less sensitive with NAA alone; the addition of myoinositol allows neurospectroscopy to achieve excellent sensitivity and specificity. In brain tumors, changes in myoinositol have been shown to be diagnostic for low-grade tumors[92–94] and taurine for differentiating medulloblastomas.[95] All of these diagnostic indicators would be missed by utilizing longer echo times. Furthermore, SNR loss also eliminates the advantage of lactate detection as shown in ►**Fig. 8**. The short-echo spectrum that shows a prominent doublet for lactate is acquired in the same lesion as a long-echo spectrum, which does not show any lactate. Indeed, most studies have concluded that short TE provides the greatest sensitivity and diagnostic value[93,96] which is supported by the ACR/ASNR recommendation to use short-echo MRS.[74]

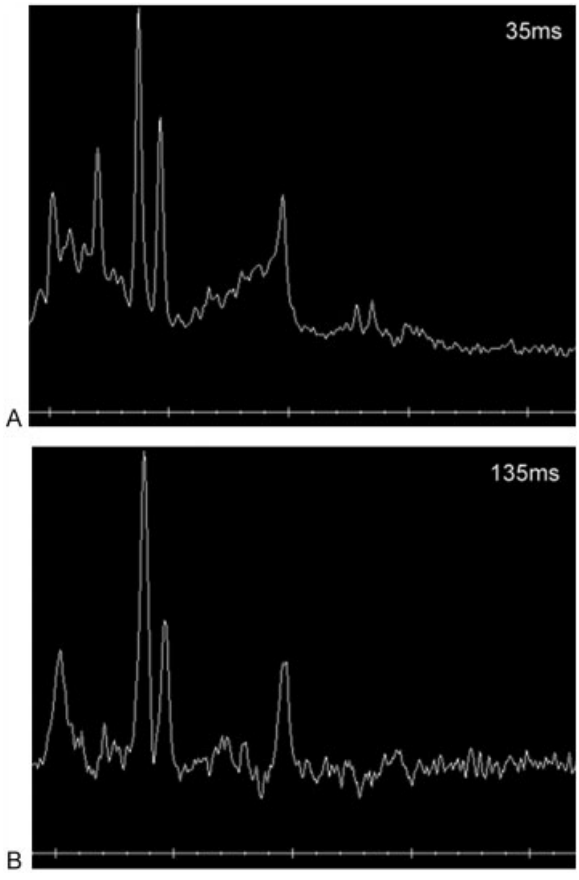

Fig. 8 Short-echo versus long-echo magnetic resonance spectroscopy. Single voxel spectra were acquired at (**A**) 35 milliseconds and (**B**) 135 milliseconds in the same lesion. The results confirm that the long-echo spectrum suffers from lower signal-to-noise ratio (SNR) when compared with the short-echo spectrum. This loss in SNR renders the lactate peak undetectable at long-echo, but readily detected in the short-echo spectrum.

PRESS versus STEAM

Point resolved spectroscopy (PRESS) and stimulated echo acquisition mode (STEAM) are the major MRS acquisition techniques that utilize 90–180–180-degree or 90–90–90-degree angles, respectively. PRESS is sometimes referred to as a spin echo sequence on some MR platforms. In the early stages of clinical MRS, STEAM MRS was used extensively given more precise localization of the 90-degree pulses; however, with time improvements have been made with PRESS MRS. Because PRESS gives almost doubled signal-to-noise advantage over STEAM, it is currently the localization sequence of choice.[7] It is important to note that metabolite peak heights and ratio will differ between PRESS and STEAM; therefore, the choice of sequence should be noted prior to data interpretation and reporting. It is important to maintain consistency in acquisition methods; hence, for all clinical protocols described in this review, the PRESS pulse sequence will be used.

Scanning Protocol

Provided with the guidelines above, the following protocols provide a step-by-step description for MRS data acquisition. The choice of voxel location will also be determined by the clinical protocol matrix described in ►**Table 2**.

Global Protocol

1. Acquire localizer images for spectroscopy: In most cases, three-dimensional magnetization prepared rapid gradient echo (3D MPRAGE) reconstructed in three planes is ideal.
2. Set up your neurospectroscopy scan parameters:
   a. Pulse sequence: PRESS
   b. TE = 35 ms
   c. TR = 2000 milliseconds (1500 ms for 1.5T)
   d. Voxel size = 2.0 cm × 2.0 cm × 2.0 cm
   e. Number of averages = 96 (128 for 1.5T)
3. Place your voxel using the landmarks:
   a. Move the ROI to location dependent on clinical indication (see ►**Table 2**)
   b. Review voxel location. Check all three planes to ensure that the voxel is positioned correctly.
4. Prescan routine:
   a. Transmitter and frequency optimization: Optimize for the greatest amount of signal and on-resonance.
   b. Water suppression: Better to slightly undersuppress than to oversuppress.
   c. Shim: This is the most critical factor, the linewidth, sometimes represented as full-width half-max (FWHM) of the water peak should be less than 14 Hz (7 Hz at 1.5T).
5. Acquire the scan.
6. Reconstruct the data. Generally, this is automated; however, the routines include spectral apodization, fast Fourier transform, baseline corrections, and peak fitting.
7. Save the data:
   a. Capture the voxel location in three planes
   b. Capture MR spectrum
   c. Export data if necessary

Focal Protocol

1. Acquire localizer images for spectroscopy:
   a. 3D MPRAGE reconstructed in three planes
   b. T1-weighted MRI pre- and postcontrast (if necessary)
2. Select your voxel location and size:
   a. Move the ROI to the lesion
      i. If lesion is unknown (i.e., query abscess, multiple sclerosis [MS] plaque, stroke), place voxel at the center of the lesion unless there is obvious necrosis
      ii. If lesion is known (i.e., tumor), place voxel at the edge of the lesion
   b. Review voxel location. Check all three planes to ensure that regions such as the skull, tissue–air interface, blood, and other problem regions are avoided.
3. Set up your neurospectroscopy scan parameters:
   a. Pulse sequence: PRESS
   b. TE = 35 ms
   c. TR = 2000 ms (1500 ms for 1.5T)
   d. Voxel size = 2.0 cm × 2.0 cm × 2.0 cm
      i. If lesion is smaller than 8 cc, start with large voxel then acquire smaller voxel. Minimum voxel size $1.2 \times 1.2 \times 1.2$ cm^3 is recommended.
   e. Number of averages = 96 (128 for 1.5T)
      i. If voxel size is reduced, increase the number of averages (avgs) accordingly (i.e., if voxel is 4 cc, increase to 256 avgs at minimum; 384 is ideal)
4. Prescan routine:
   a. Transmitter and frequency optimization: Optimize for the greatest amount of signal and on-resonance.
   b. Water suppression: Better to slightly undersuppress than to oversuppress.
   c. Shim: This is the most critical factor, the linewidth, sometimes represented as full-width half-max (FWHM) of the water peak should be less than 14 Hz (7 Hz at 1.5T).
5. Acquire the scan.
6. Optional: Chemical shift imaging:
   a. Prescribe the excitation volume voxel around the area of interest (i.e., lesion) and the area surrounding it. Use the same center slice as that of the single voxel exam. Use the same care described above in not placing the excitation volume too close to the skull and other areas of inhomogeneity.
   b. If available, place saturation bands over skull closest to the voxel to avoid any lipid contamination. Make sure that the saturation bands do not intersect with the excitation volume. The sat bands are used to cut out the residual water and any lipids surrounding the skull. Note that sat bands surrounding the voxel already exist; therefore, use the additional sat bands at different angles (see ►**Fig. 9**).
   c. Recommended parameters:
      i. Pulse sequence: PRESS-CSI
      ii. TE = 35 ms
      iii. TR = 1000 ms
      iv. Phase encode = 24
      v. Frequency encode = 24
      vi. Field of view = 24 × 24 cm
      vii. Slice thickness = 10 mm
      viii. NEX = 1

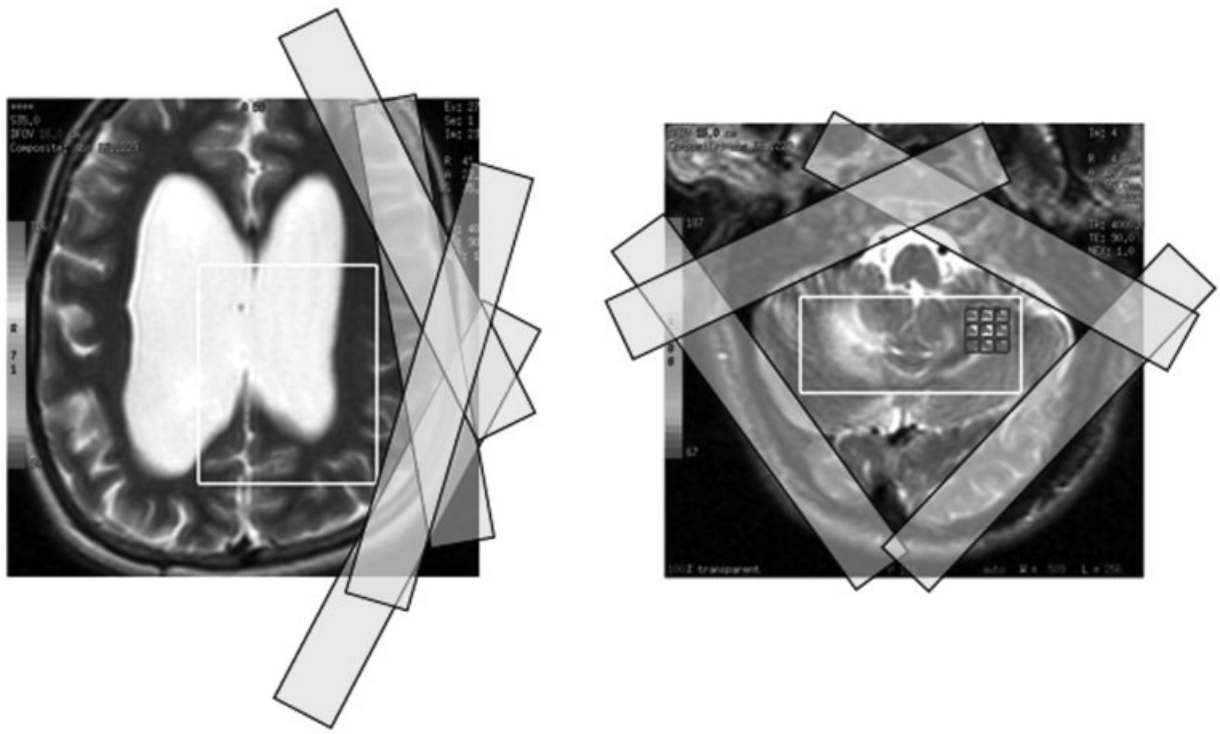

Fig. 9 Saturation band placement. Two examples of outer volume saturation bands placed in a chemical shift imaging acquisition. In the first example (left), the saturation bands are placed along the left side of the skull to avoid lipid contamination. In the second example (right), the saturation bands are placed along the bones of the posterior fossa to limit lipid contamination of a cerebellar lesion.

7. Reconstruct the data. Generally, this is automated; however, the routines include spectral apodization, fast Fourier transform, baseline corrections, and peak fitting.
8. Save the data:
   a. Capture the voxel location in three planes (see ►**Fig. 10** for CSI data capture)
   b. Capture MR spectrum (see ►**Fig. 10** for CSI data capture)
   c. Export data if necessary

Shimming

As discussed previously in voxel positioning, one of the main goals of these methods is to optimize homogeneity and avoid susceptibility artifacts to obtain spectra of the quality shown in ►**Figs. 2** and **5**. However if homogeneity is not optimized, the results can be disastrous as shown in ►**Fig. 6**. ►**Figure 6c** provides an example of a poor shim where the linewidths of the peaks are broad, such that choline and creatine overlap one another and the Glx region is a broad resonance instead of separate multiplets as seen in the other examples. As a result, it becomes difficult to distinguish the peaks and can affect the diagnosis. Therefore, to minimize these artifacts, an additional step prior to data acquisition is to shim the MRS voxel region. This is the process by which the B_0 field is made as homogeneous as possible by using the x-, y-, and z-gradient coils.

All MR platforms have automated shimming routines that remove the manual and time-consuming steps required for shimming. However, it is important for the operator to make a note of whether the shim was successful. To determine this, a measure of the water peak linewidth needs to be recorded. On GE platforms, this is determined after the auto prescan and appears in the control window and reported as "FWHM" or "Linewidth." At 3.0T, a linewidth of less than 14 Hz is desired (7 Hz at 1.5T). This is equal to 0.01 ppm on the MRS scale and implies that one can distinguish peaks with that level of spectral resolution. On Siemens platforms, this number is obtained in the "Adjustments" window under the "Interactive Shim" tab after clicking on the "Measure." On Siemens 3.0T, a linewidth of less than 20 Hz is desired as the water peak is expressed in magnitude mode, which is inherently broader. If the desired linewidth is not achieved, run through the automated prescan routines again. If the second attempt is not successful, return to voxel positioning and move the voxel away from regions that may cause heterogeneity and repeat. Although this may be somewhat laborious, it is critical to the success of a clinical neurospectroscopy program and will guarantee excellent technical quality from which you can reliably report the spectrum.

Reporting MRS

Postprocessing

Although several third-party MRS postprocessing packages such as LC model[97] and JMRUI[98] are available and widely used by the MRS research community, the software packages

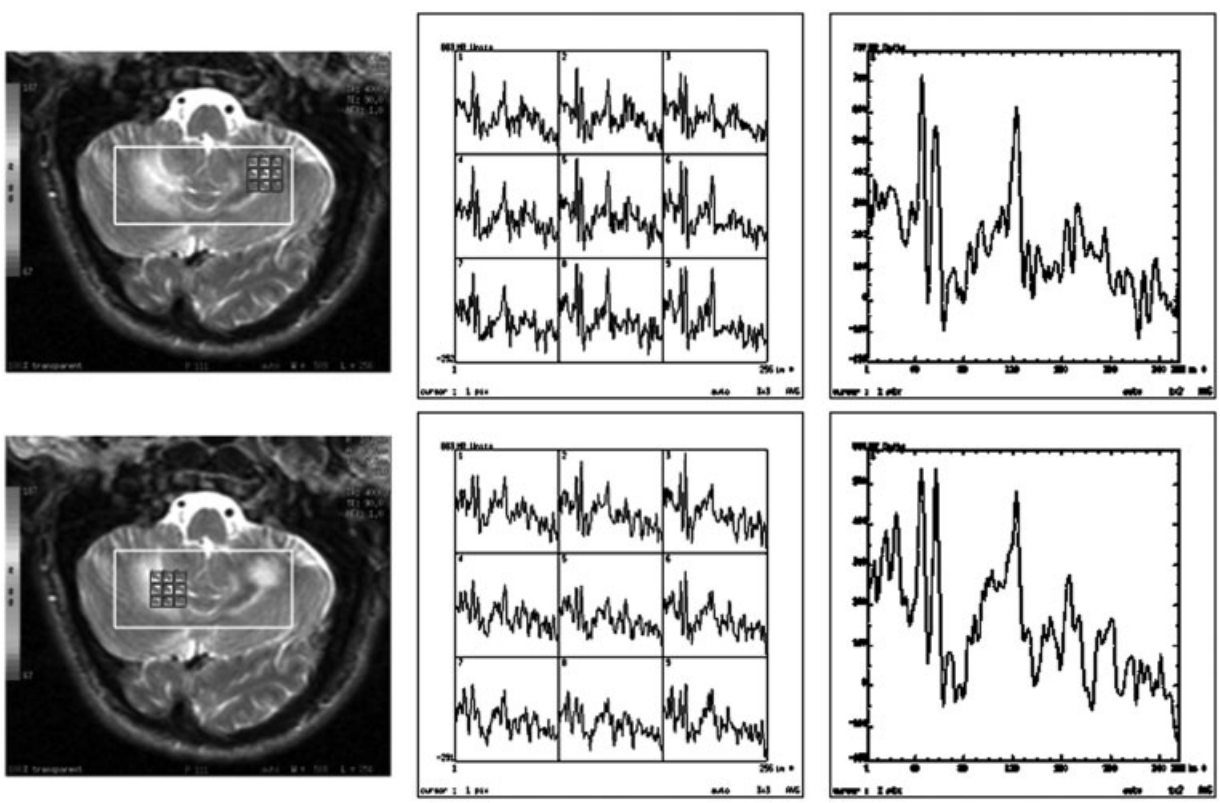

Fig. 10 Chemical shift imaging (CSI) data display. An example of how to reconstruct CSI data for rapid visual analysis. A region of interest is selected within the excitation volume (white box) on the magnetic resonance image (left) and individual spectra are displayed (middle) as well as the summed spectra (right). This allows the radiologist to rapidly peruse the summed spectra for those that are of interest and examine the spatial localization of metabolic changes in the individual spectra.

themselves are not FDA-approved; therefore, they cannot be integrated into the MR scanner for clinical reporting of the MRS results. All MR platforms can produce a spectrum and numerical results for clinical reporting; however, the methodology and results are highly specific to the manufacturer and scanner model. As a result, there are several different levels at which one can interpret and report the MRS results.

The most basic approach is by visual inspection of the spectrum. For focal changes, such as identifying increased choline or myoinositol, or the presence of additional metabolites in abscesses, this method is sufficient. In the following section, we will describe the metabolites in the spectrum and their pathophysiologic role and how they can be utilized for clinical diagnosis. The second level of postprocessing involves the generation of metabolite ratios (i.e., NAA/Cr, Cho/Cr, mI/Cr), which can be readily generated from the software packages available across all MR manufacturing platforms or from visual inspection as well. In our spectroscopy courses, all attendees are taught to read a spectrum and generate ratios by visual inspection, which are remarkably comparable to the computer-generated results. Finally, if the resources are available to the clinician, the more-advanced spectroscopy packages such as the LC model can be utilized for generating "absolute" concentrations.

Postprocessing of CSI results also differs significantly between MR platforms. One of the difficulties of interpreting CSI results is that the spectrum from each voxel must be evaluated individually, which can be time consuming. Although it is tempting to utilize the metabolite maps in its place, the spatial resolution of the metabolite maps is interpolated, which may result in overinterpretation of lesion boundaries. There are also issues with signal correction where some areas may appear to have increased SNR, but overall signal may be increased in that region, leading to possible misinterpretation of the data.

We advocate viewing the spectral results using a method that is not as time-consuming as analyzing each spectrum. ►**Figure 10** shows a sample CSI output where a region of the CSI volume is selected and the individual spectra from that region are shown. In addition, a summed spectra of all of the spectra from that region is obtained. This procedure is repeated at multiple regions in the CSI volume. The major advantage of CSI is that in postprocessing the ROI can be readily shifted to any location with the excitation volume. The radiologist then just examines the summed spectra; those spectra that appear to have significant changes are then examined in more detail. This enables a rapid yet thorough analysis of the CSI data.

Data Interpretation

Metabolites and Their Roles in Disease Diagnosis

Lipids

Lipids are broad peaks that occur at 0.9 and 1.2 ppm. In healthy tissues, there should be very little lipid in the spectrum unless the voxel is placed too close to the skull, whereby the lipid signal from subcutaneous fat in the skull would dominate the spectrum. The presence of lipid can have diagnostic value in brain tumors where lipid indicates necrosis,[99] or in brain injury where lipid is indicative of neuronal damage.[100]

Lactate

Lactate is generally seen as a doublet (two peaks close together) at a frequency of 1.33 ppm. Again, healthy tissue does not have sufficient lactate to be detectable with MRS. However, CSF contains some lactate, so that if the voxel is placed entirely in the ventricle lactate may appear in the spectrum. Lactate as a product of anaerobic glycolysis is detected in diseased brain when oxygen starved. It is of great diagnostic value in cases of hypoxia,[30] brain injury,[76] and stroke.[31] It is also elevated in some tumors, where it is suggestive of aggressiveness,[101] as well as abscesses.[66]

N-Acetylaspartate

At 2.0 ppm, N-acetylaspartate (NAA) is an amino acid derivative synthesized in neurons and transported along axons. It is therefore a "marker" of viable neurons, axons, and dendrites.[27] The diagnostic value of NAA lies in the ability to quantify neuronal injury or loss on a regional basis; therefore, decreased NAA plays a diagnostic role in brain tumors, head injury, dementias, and many other neurologic disorders where neuronal loss is expected. Increased NAA is observed only in recovery and in Canavan's disease, which is due to a specific genetic disorder that reduces NAA-deacylase activity resulting in net accumulation of NAA.[102]

Glutamate—Glutamine—Gamma-aminobutyrate (Glx)

A mixture of closely related amino acids, amines, and derivatives involved in excitatory neurotransmission lie between 2.1 and 2.4 ppm. Glutamate—glutamine—gamma-aminobutyrate (Glx) is a vital marker in MRS of stroke, lymphoma, hypoxia, and many metabolic brain disorders.[103]

Creatine

The primary resonance of creatine (Cr) lies at 3.0 ppm. It is the central energy marker of both neurons and astrocytes and remains relatively constant. For that reason, it is often used as an internal reference for comparison to other metabolites. Although some studies have found Cr reduced, it is only in inborn errors of metabolism where significant reductions of Cr occur.[104]

Choline

Choline (Cho) includes several soluble components of brain myelin and fluid-cell membranes that resonate at 3.2 ppm. Because by far the majority of choline-containing brain constituents are not normally soluble, pathologic alterations in membrane turnover (tumor, leukodystrophy, multiple sclerosis) result in a massive increase in MRS-visible Cho.[105]

Myoinositol

A little-known polyol (sugar-like molecules) that resonates at 3.6 ppm, myoinositol (mI) is mostly a diagnostic "modifier" in those diseases that affect Cho (tumor, MS, etc.). As an astrocyte marker and osmolyte, mI contributes specificity

in dementia diagnoses,[106] and an almost absolute specificity to hepatic encephalopathy and hyponatremic brain syndromes.[25]

Additional Resonances

Several additional brain metabolites can be measured with MRS, such as gamma-aminobutyric acid (GABA), scylloinositol, glutathione, etc.; however, specialized editing sequences or additional software is required to detect and measure them; therefore, they are outside the scope of typical clinical practice. However, as MRS methods mature, they may soon be available to clinicians to assay.

Hunter's Angle

Named for an eminent neurosurgeon who applied a pocket comb to the task of recognizing the 45-degree angle formed by the peaks mI, Cr, Cho, and NAA, when they are present in normal proportions: NAA/Cr ~ 1.5; Cho/Cr ~ 0.75; mI/Cr ~ 0.5 as shown in ►**Fig. 11**. This method provides a very rough-and-ready approach for quick visual analysis of a spectrum. ►**Figure 12** illustrates several examples where Hunter's angle (HA) can be applied: In brain tumors due to the increased Cho and decreased NAA, HA is "reversed" or -45 degrees, demonstrating a clear difference between tumor spectra and normal spectra. Similarly, in Alzheimer's disease, HA is flat, 0-degrees due to the increase in mI and decrease in NAA. As with any simple methodology, there are exceptions to the rules: This method was originally designed for examining STEAM spectra. PRESS spectra have higher Cho peak heights, and hence do not line up as cleanly although the overall approach still holds. This method is also very location dependent as other brain regions such as the midbrain have normally high levels of choline. This method also does not apply to long-echo MRS. Nonetheless, it provides a rapid approach to visualizing spectra.

Pattern Recognition for the Physician

Although there are a number of highly sophisticated pattern recognition methods using computational methods (i.e., the European INTERPRET/eTUMOR multicenter study[107]), one should not underestimate the innate pattern recognition abilities of the physician. One effective method developed in our course was the use of an identification chart that was posted in each reading room, which provided sample spectrum from a range of different diseases that could be used for rapid comparison with the acquired data. We have provided an updated version of this MRS chart to include healthy control, focal spectroscopy, and sample global spectroscopy results that may be useful to the reader in ►**Fig. 12**. There are also numerous reviews that provide examples of spectra as well as textbooks that can provide additional information.

Normative Database

For global spectroscopy, the metabolites described above are measured and compared against a normative database

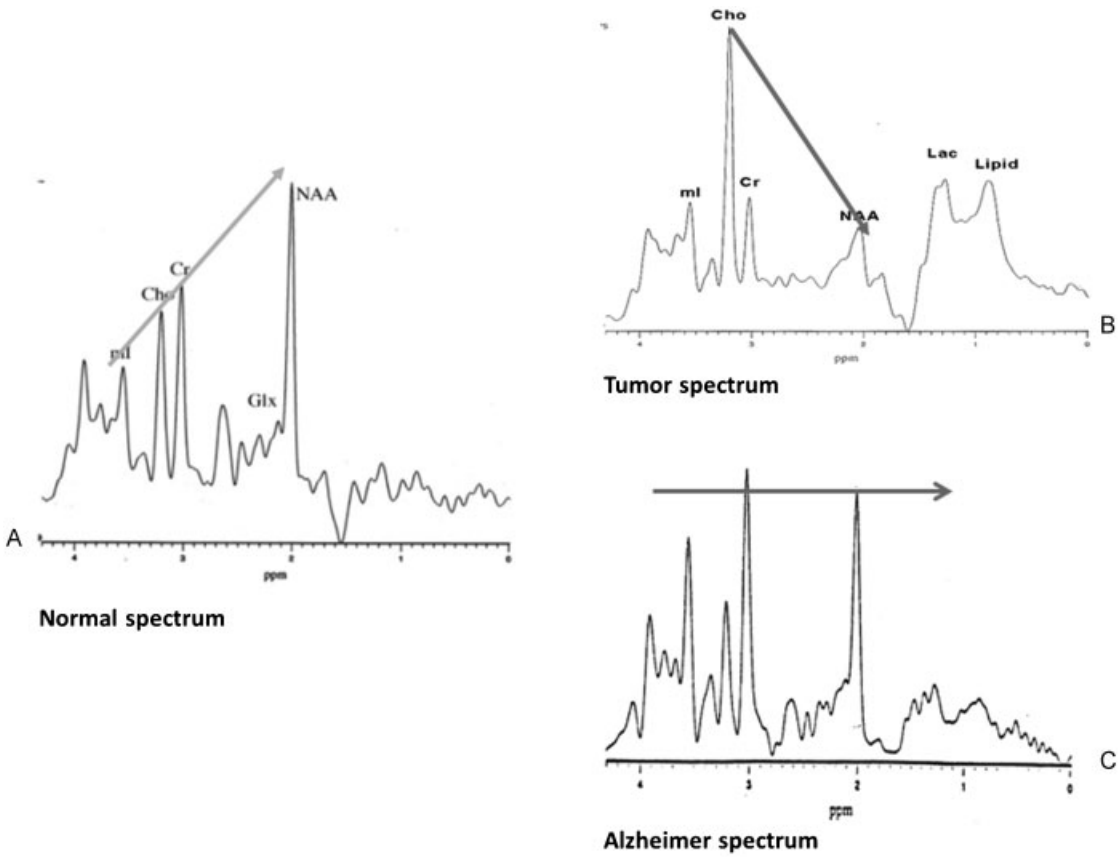

Fig. 11 Hunter's angle. Examples of Hunter's angle in (**A**) spectra obtained from healthy control in comparison to (**B**) brain tumor and (**C**) the posterior gray matter of a patient with Alzheimer's disease.

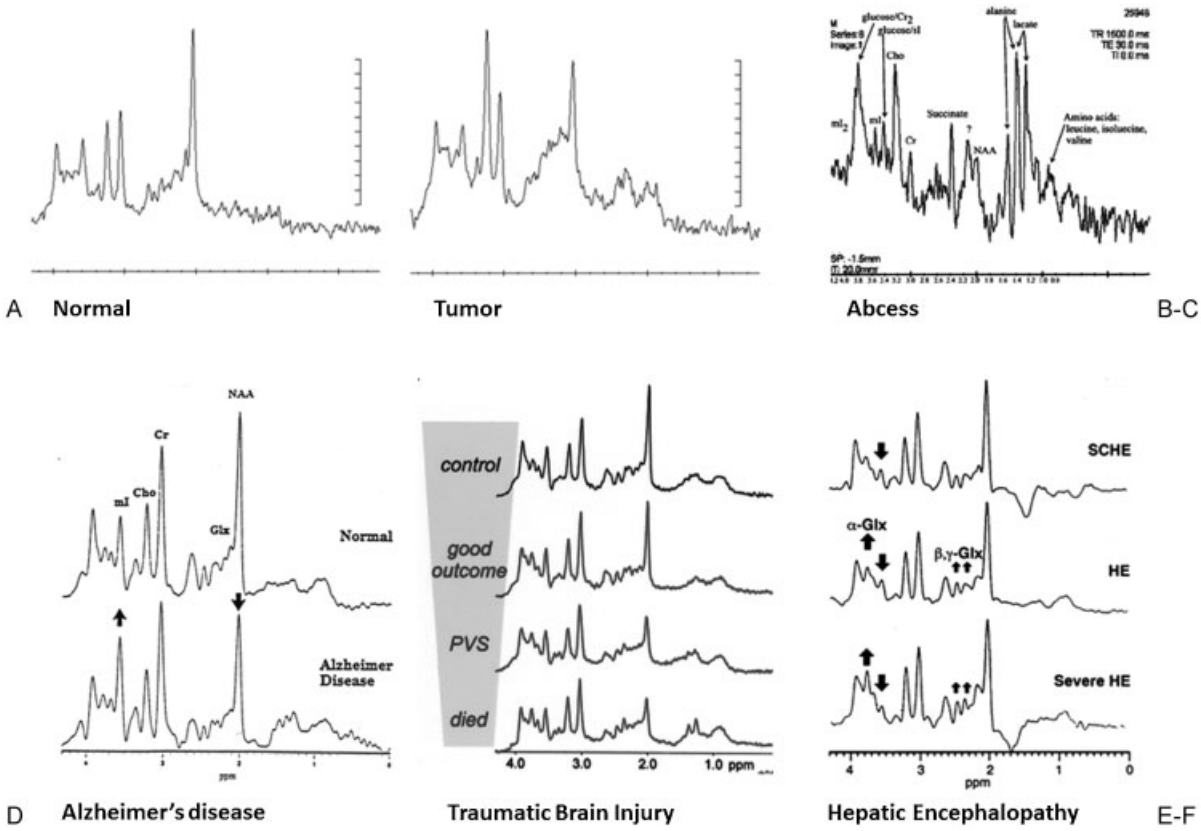

Fig. 12 Identification chart of magnetic resonance spectroscopy (MRS) in neurologic diseases. Representative spectra are shown from (**A**) parietal white matter of a healthy control, (**B**) voxel at the edge of a glioblastoma, (**C**) voxel in an abscess (neurocysticercosis). The bottom row shows spectra acquired from the posterior gray matter in different global neurologic diseases. (**D**) Healthy age-matched control (top) and a patient with severe Alzheimer's disease. (**E**) Spectra acquired from healthy control (top), a patient with good outcome (middle top), a patient in persistent vegetative state (PVS; middle bottom), and a patient who died (bottom) after head injury. Spectra were all acquired 4 days after the insult. The results demonstrate that MRS can predict outcome in brain injury. (**F**) Grading of hepatic encephalopathy from subclinical hepatic encephalopathy (SCHE; top) where MRS changes precede clinical changes; diagnosed hepatic encephalopathy (HE; middle), and severe HE (bottom).

of values. While we have described straightforward standard MRS protocols and methods for interpreting the data, the ultimate means of utilizing MRS is to take advantage of the quantitative nature of MRS and compare patient results with data from healthy control subjects from a normative database. It is often suggested that clinical sites develop their own normative databases but this is not a trivial task and presents yet another hurdle for the clinical adoption of MRS. We therefore present the following study which examines the reproducibility of the protocol described in this review by measuring differences between different scanner platforms and sites as well as measuring reproducibility and test-retest reliability to demonstrate that the methods described are robust and readily reproduced by all sites.

Scan Protocol

Twenty-seven normal subjects (age 22–39) were examined on three different clinical scanners (GE HDx, Siemens TIM Trio, Philips Achieva), all employing single-voxel MRS technique, TE 35 ms, and 3 Tesla. The voxel size was $2 \times 2 \times 2\ cm^3$ for the Siemens and GE scanners as shown in ►**Fig. 3**, but $2.5 \times 2.5 \times 2.9\ cm^3$ for Philips (►**Fig. 13**) in the posterior GM region. All subjects gave informed consent, and subject information was made anonymous. These studies were approved by the internal review boards with informed consents, and were compliant with HIPAA (Health Insurance Portability and Accountability Act) regulations.

Seven healthy young subjects were examined on a clinical GE 3T scanner using a 12-channel volume head coil. Ten subjects were examined on a Siemens 3T scanner using an eight-channel volume head coil. Ten other subjects were examined on a Philips 3T using an eight-channel head coil. In each subject, standard three-plane and high-resolution images were acquired for anatomic localizations followed by 1H MRS. Shimming values for MRS were recorded to ensure sufficient linewidth (< 14 Hz) and water suppression. Three MRS data points were acquired as follows: the first two scans (Scans 1 and 2) were consecutively acquired with the same shim for test-retest purposes, and the third (Scan 3) was acquired after voxel relocation (in the same posterior GM region) to demonstrate reproducibility. The raw data files were then transferred to a dedicated computer where the LC model[97] was employed for data processing.

Data Processing and Statistics

To ensure identical, observer-independent analysis, metabolic ratios were determined at a central data processing site

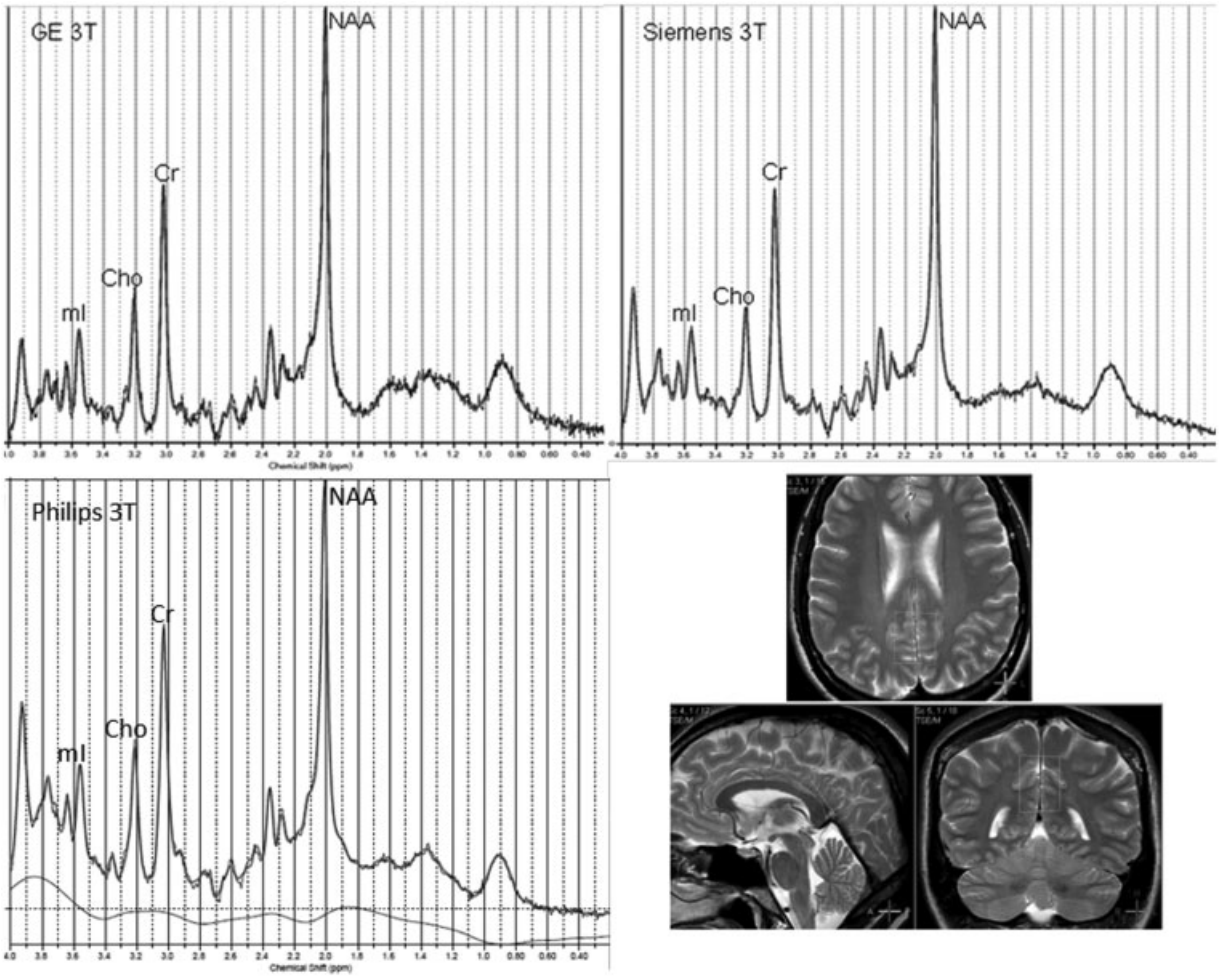

Fig. 13 Comparison of magnetic resonance spectroscopy of different manufacturers. Representative data from a subject acquired on GE 3T Siemens 3T (top right), and Philips 3T (bottom left). Note that the voxel size for GE 3T and Siemens 3T were the same (see ►**Figure 3**); however, the voxel size for the Philips 3T was different and is shown in the bottom right panel. (NAA, N-acetylaspartate; Cho, choline; Cr, creatine; mI, myoinositol)

after analysis of all data with the LC model. The raw data file was loaded into the LC model program, which fits the data with a basis set for each scanner and provides metabolic ratios of interest, namely, NAA, choline (Cho), and myoinositol (mI), using creatine (Cr) as a reference. Percent differences for scans within each subject were also calculated to determine reproducibility of each scanner. Student *t* tests were applied to compare each metabolic ratio in different field strengths and vendors.

Results

Representative metabolic profiles from each of the scanners used are shown in ►**Fig. 13**. The metabolic ratios NAA/Cr, Cho/Cr, mI/Cr, and NAA/mI are shown in ►**Table 3** (mean ± standard deviation [SD]). The percent differences in the ratios between vendors at the same field strength and voxel size (Siemens 3T vs GE 3T) are 1.45% for NAA/Cr, 0% for Cho/Cr, 5.95% for mI/Cr, and 7.34% for NAA/mI. As expected the ratios for NAA, Cho, and mI are significantly different between the

Table 3 Metabolic Ratios Measured with Each Scanner

	Metabolic Ratios (mean ± SD)			
Scanner (# of subjects)	NAA/Cr	Cho/Cr	mI/Cr	NAA/mI
Siemens 3T ($N = 13$)	1.36 ± 0.11	0.19 ± 0.01	0.84 ± 0.08	1.64 ± 0.22
GE 3T ($N = 7$)	1.38 ± 0.07	0.19 ± 0.01	0.79 ± 0.07	1.77 ± 0.17
Philips 3T ($N = 10$)	1.20 ± 0.05	0.18 ± 0.01	0.80 ± 0.06	1.50 ± 0.13

Abbreviations: NAA, N-acetylaspartate; Cho, choline; Cr, creatine; mI, myoinositol.

Table 4 Percent Differences Calculated for Test-Retest and Voxel Replacement

		Percent Differences for Each Metabolite			
		(NAA/Cr)	(Cho/Cr)	(mI/Cr)	(NAA/mI)
Test-Retest	Siemens 3T	2.39	2.54	5.11	5.67
(Scan 1 vs Scan 2)	GE 3T	2.19	3.58	7.00	6.54
Voxel Replacement	Siemens 3T	3.36	5.24	6.02	6.17
(Scan 1 vs Scan 3)	GE 3T	2.84	4.76	6.29	5.38

Abbreviations: NAA, N-acetylaspartate; Cr, creatine; Cho, choline; mI, myoinositol.

Philips data and the GE and Siemens data because a different voxel size was used. It should be noted that there were no significant differences between Siemens and GE data ($p > 0.05$) demonstrating that rigorous attention to protocol will ensure the best reproducibility. The Cho/Cr ratio is the most stable across the board for all vendors. ►**Table 4** lists the means of the percent difference between the two test-retest scans, and between the first scan and third scan after the voxel was relocated. NAA/Cr demonstrates the smallest percent differences, at 2.12 to 3.36% for all scanners in both comparisons. The percent differences in the Cho/Cr ratio between individual scans were higher than for the NAA/Cr ratio. The mI/Cr ratio showed larger differences between 5 to 7%, which may be attributed to the "collapse" of the peak due to its multiplet resonance structure at 3T.[108]

Reporting MRS Results

One of the key lessons learned early on at the clinical MRS service at Huntington Medical Research Institutes was that one or two line comments about the MRS results were not sufficient for insurance companies to reimburse for MRS. Unfortunately, at many sites, this continues to be common practice where MRS is just an add-on to the report and as a result reimbursement for MRS has been problematic. Instead, we developed a systematic approach to reporting MRS that provides a full-page report of the MRS results based on a template. An example of an actual patient report (redacted for personal health information) is shown in ►**Fig. 14**. The following steps are then taken to generate the report:

Clinical Information

Just as with any MRI report, the template includes patient information, date of exam, clinical indications, etc.

MRI and MRS Methods

Similar to MRI reports, the pulse sequences are described in detail including echo time, pulse sequence, and voxel location.

MRI Results

To prevent overlap with the MRI report, MRI results are reported in less detail with results that only pertain to the MRS acquisition.

MRS Results

The reporting template provides a section for each voxel location. The patient's metabolite ratios are reported with respect to creatine and include NAA, Cho, and mI. Glx values are not reported, only noteworthy increases or decreases to that region are noted. In this case, Glx was normal and therefore nothing is reported. Key to this report is the normal data presented below the patient value. Much like a blood test, the comparison of the patient's value can then be readily compared with the values from the normative database. In other versions of the reporting template, the standard deviation and normal range of the control data were also reported.

MRS Interpretation

The following steps were then rigorously followed for each voxel:

1. Provide acquisition details—Voxel size and sequence parameters should be indicated.
2. Technical quality assessment—The first line of the report should comment on any potential technical issues with the data acquisition. The report should consider SNR and the presence of any artifacts in the spectrum. Technical quality is rated as "Excellent," "Good," and "Poor" with explanations for poor quality and confidence of interpretation.
3. Lipid/lacate assessment—Determine if there is lipid and/or lactate. If so, comment on the pathophysiologic origin.
4. Ratio assessment—Starting with NAA/Cr, describe if the patient's metabolite value is within normal variation, which we generally considered within two standard deviations of the mean of the normal control data. As a result, the sensitivity of the methodology is therefore highly dependent upon the variability and reproducibility of each metabolite as described above. If the patient's value is outside of two standard deviations, indicate whether it is increased or decreased and describe the difference with respect to the mean of the healthy controls (e.g., 10% increased). Repeat for each metabolite in order from right to left. By being systematic, each resonance will be evaluated.

Impression

In this section, the MRI and MRS findings are summarized and an evaluation of results within the context of the clinical indication is provided. If previous exams were completed, the

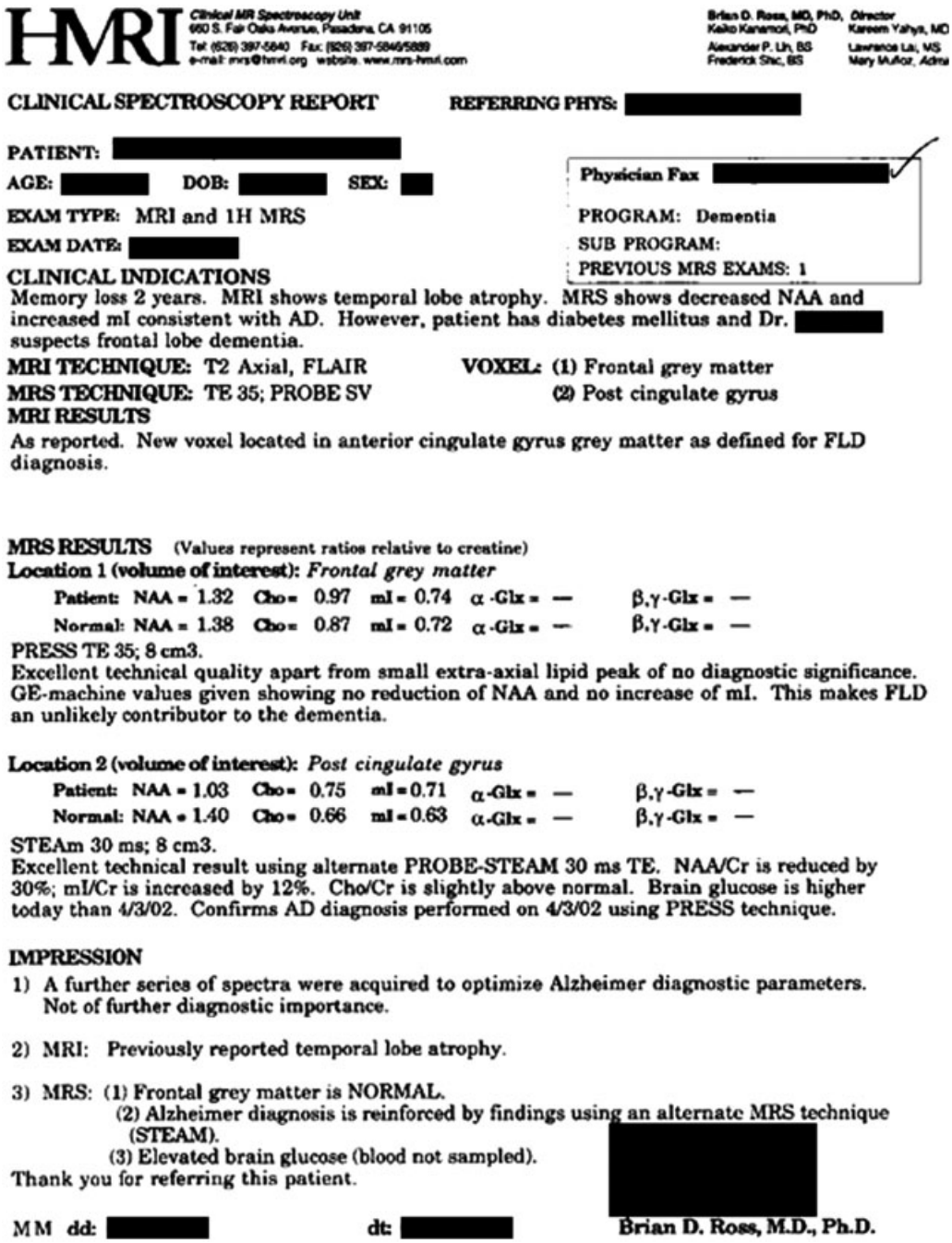

HMRI Clinical MR Spectroscopy Unit
950 S. Fair Oaks Avenue, Pasadena, CA 91105
Tel: (626) 397-5640 Fax: (626) 397-5846/5889
e-mail: mrs@hmri.org website: www.mrs-hmri.com

Brian D. Ross, MD, PhD, Director
Keiko Kanamori, PhD Kareem Yahya, MD
Alexander P. Lin, BS Lawrence Lai, MS
Frederick Shic, BS Mary Muñoz, Admin

CLINICAL SPECTROSCOPY REPORT REFERRING PHYS: [redacted]

PATIENT: [redacted]
AGE: [redacted] DOB: [redacted] SEX: [redacted]
EXAM TYPE: MRI and 1H MRS
EXAM DATE: [redacted]

Physician Fax [redacted]
PROGRAM: Dementia
SUB PROGRAM:
PREVIOUS MRS EXAMS: 1

CLINICAL INDICATIONS
Memory loss 2 years. MRI shows temporal lobe atrophy. MRS shows decreased NAA and increased mI consistent with AD. However, patient has diabetes mellitus and Dr. [redacted] suspects frontal lobe dementia.

MRI TECHNIQUE: T2 Axial, FLAIR
MRS TECHNIQUE: TE 35; PROBE SV
VOXEL: (1) Frontal grey matter
(2) Post cingulate gyrus

MRI RESULTS
As reported. New voxel located in anterior cingulate gyrus grey matter as defined for FLD diagnosis.

MRS RESULTS (Values represent ratios relative to creatine)
Location 1 (volume of interest): *Frontal grey matter*

Patient:	NAA = 1.32	Cho = 0.97	mI = 0.74	α-Glx = —	β,γ-Glx = —
Normal:	NAA = 1.38	Cho = 0.87	mI = 0.72	α-Glx = —	β,γ-Glx = —

PRESS TE 35; 8 cm3.
Excellent technical quality apart from small extra-axial lipid peak of no diagnostic significance. GE-machine values given showing no reduction of NAA and no increase of mI. This makes FLD an unlikely contributor to the dementia.

Location 2 (volume of interest): *Post cingulate gyrus*

Patient:	NAA = 1.03	Cho = 0.75	mI = 0.71	α-Glx = —	β,γ-Glx = —
Normal:	NAA = 1.40	Cho = 0.66	mI = 0.63	α-Glx = —	β,γ-Glx = —

STEAm 30 ms; 8 cm3.
Excellent technical result using alternate PROBE-STEAM 30 ms TE. NAA/Cr is reduced by 30%; mI/Cr is increased by 12%. Cho/Cr is slightly above normal. Brain glucose is higher today than 4/3/02. Confirms AD diagnosis performed on 4/3/02 using PRESS technique.

IMPRESSION
1) A further series of spectra were acquired to optimize Alzheimer diagnostic parameters. Not of further diagnostic importance.
2) MRI: Previously reported temporal lobe atrophy.
3) MRS: (1) Frontal grey matter is NORMAL.
(2) Alzheimer diagnosis is reinforced by findings using an alternate MRS technique (STEAM).
(3) Elevated brain glucose (blood not sampled).

Thank you for referring this patient.

[redacted]

MM dd: [redacted] dt: [redacted] Brian D. Ross, M.D., Ph.D.

Fig. 14 Sample magnetic resonance spectroscopy report. Sample report redacted to remove personal health information.

results should be compared with previous results. Depending on the clinical indication, the differences in the metabolite ratios from the normative database will provide the answers to the clinical question. In this particular case, there was a question of whether the patient had Alzheimer's disease or frontal lobe dementia. The frontal lobe MRS results were within normal range; therefore, the conclusion is likely not frontal lobe dementia. However, there is clear evidence of increased mI and decreased NAA in the posterior GM, which is indicative of Alzheimer's disease and consistent with the previous findings.

Similar reports can be generated for focal disease where comparisons can be made to GM or WM normative values or the contralateral voxel. Quality assessment as well as metabolite ratios would then be reported and results such as increased Cho would confirm evidence of tumor. If CSI was acquired in the same exam, the first step would be to create a summed spectra from the same region of interest that the SVS scan was obtained. This provides quality control for CSI exams as the summed spectra should be very comparable to the SVS scan. If the technical quality is sound, then areas of increased Cho are reported within the CSI volume. This presents the

ideal solution by combining the robust SVS acquisition with the spatially encoded CSI acquisition.

MRS in the Clinic

Reimbursement

Although Medicare has determined MRS to be investigational, other insurance carriers, including Cigna[109] and Blue Cross/Blue Shield in over 20 states including Colorado, Connecticut, Georgia, Indiana, Kentucky, Maine, Missouri, Nevada, New Hampshire, Ohio, Virginia, Wisconsin,[110] Delaware,[111] Michigan,[112] New York,[113] and West Virginia,[114] all reimburse MRS for tumor diagnosis under CPT 76390. Some also reimburse for inborn errors of metabolism and leukoencephalopathies.[115] Clearly, spectroscopy is still reimbursable and in fact a position statement from Cigna Healthcare states, "Although supporting data are lacking in the form of well-designed, large-population, multi-center controlled clinical trials, results reported from a number of small case series and trials, as well as information in review literature, indicate that MRS has become standard of care as an effective imaging technique for the diagnosis, treatment and monitoring of patients with brain lesions." This position statement takes into account both the ARHQ and BC/BS technology assessments and still considers MRS reimbursable for brain tumor diagnosis. The global fee set by CMS for MRS in 2011 is 10.78 relative value units, equivalent to $572.42.[116] In 2009, we conducted a survey of reimbursement for CPT 76390 from medical billers from across the country and have found that the average rate of reimbursement is $587.49.[117] It is important to note, however, that one must adopt a proactive reimbursement strategy. First, it is common that initial billing submissions will be rejected by the payers. These rejections must be challenged, and it is important to educate the payer of the value and medical necessity of MRS in each case. Second, spectroscopy should not be a one- to two-line "add-in" to a radiology report, a separate report should be issued that clearly indicates the diagnostic value of the MRS exam and provides quality assurance and a comparison of normal age-matched metabolite levels. Finally, high-quality data acquisition and reproducible spectroscopy protocols for disease diagnosis as described in this review are critical for maintaining excellence to ensure billing reimbursement.

Future Directions

Despite a large literature suggesting the promise of MRS for routine clinical practice, there remains skepticism and lack of broad acceptance of a proven technology. We believe that the present review challenges that prevailing perception and offers a straightforward standard MRS protocol that can be adopted by any potential clinical or research investigator user of MRS. To be standard, the protocol should be applicable to widely available commercial MR scanners, in diverse geographical locations, and employ either of the two currently standard field strengths. Although consensus on the standardized protocol needs to be reached, we hope that this article provides some guidelines for such an endeavor.

What is the next step for MRS? Fryback and Thornbury advocate the use of six criteria for evidence-based evaluation of imaging modalities: technical feasibility, diagnostic accuracy, diagnostic impact, therapeutic impact, outcome impact, and societal impact.[118] Prior studies have amply demonstrated that MRS can fulfill the first two criteria; however, few studies have demonstrated that MRS changes diagnostic thinking, or changes the patient's therapy and outcome, none have measured the societal impact (i.e., cost-benefit).[1] It is critical that the MRS community now focus on studies that quantify the extent to which MRS provides better diagnosis, leads to changes in therapy, and improves patient outcomes. Ultimately, this would be best measured by a formal cost-benefit analysis of these well-established MRS procedures.

References

1 Lin AP, Tran TT, Ross BD. Impact of evidence-based medicine on magnetic resonance spectroscopy. NMR Biomed 2006;19(4):476–483
2 Ross B, Bluml S. Magnetic resonance spectroscopy of the human brain. Anat Rec 2001;265(2):54–84
3 Tran T, Ross B, Lin A. Magnetic resonance spectroscopy in neurological diagnosis. Neurol Clin 2009;27(1):21–60, xiii xiii
4 Xu V, Chan H, Lin AP, et al. MR spectroscopy in diagnosis and neurological decision-making. Semin Neurol 2008;28(4):407–422
5 Zhu H, Barker PB. MR spectroscopy and spectroscopic imaging of the brain. Methods Mol Biol 2011;711:203–226
6 Alger JR. Quantitative proton magnetic resonance spectroscopy and spectroscopic imaging of the brain: a didactic review. Top Magn Reson Imaging 2010;21(2):115–128
7 Drost DJ, Riddle WR, Clarke GD; AAPM MR Task Group #9. Proton magnetic resonance spectroscopy in the brain: report of AAPM MR Task Group #9. Med Phys 2002;29(9):2177–2197
8 Law M. MR spectroscopy of brain tumors. Top Magn Reson Imaging 2004;15(5):291–313
9 Castillo M, Kwock L, Scatliff J, Mukherji SK. Proton MR spectroscopy in neoplastic and non-neoplastic brain disorders. Magn Reson Imaging Clin N Am 1998;6(1):1–20
10 Gillies RJ, Morse DL. In vivo magnetic resonance spectroscopy in cancer. Annu Rev Biomed Eng 2005;7:287–326
11 McIntyre DJ, Madhu B, Lee SH, Griffiths JR. Magnetic resonance spectroscopy of cancer metabolism and response to therapy. Radiat Res 2012;177(4):398–435
12 Sibtain NA, Howe FA, Saunders DE. The clinical value of proton magnetic resonance spectroscopy in adult brain tumours. Clin Radiol 2007;62(2):109–119
13 Negendank W. Studies of human tumors by MRS: a review. NMR Biomed 1992;5(5):303–324
14 Howe FA, Opstad KS. 1H MR spectroscopy of brain tumours and masses. NMR Biomed 2003;16(3):123–131
15 Hollingworth W, Medina LS, Lenkinski RE, et al. A systematic literature review of magnetic resonance spectroscopy for the characterization of brain tumors. AJNR Am J Neuroradiol 2006;27(7):1404–1411
16 Cecil KM, Lenkinski RE. Proton MR spectroscopy in inflammatory and infectious brain disorders. Neuroimaging Clin N Am 1998;8(4):863–880
17 Chang L, Ernst T. MR spectroscopy and diffusion-weighted MR imaging in focal brain lesions in AIDS. Neuroimaging Clin N Am 1997;7(3):409–426

18 Kapsalaki EZ, Gotsis ED, Fountas KN. The role of proton magnetic resonance spectroscopy in the diagnosis and categorization of cerebral abscesses. Neurosurg Focus 2008;24(6):E7
19 Kuzniecky R. Clinical applications of MR spectroscopy in epilepsy. Neuroimaging Clin N Am 2004;14(3):507–516
20 Ranjeva JP, Confort-Gouny S, Le Fur Y, Cozzone PJ. Magnetic resonance spectroscopy of brain in epilepsy. Childs Nerv Syst 2000;16(4):235–241
21 Ross BD, Bluml S, Cowan R, Danielsen E, Farrow N, Tan J. In vivo MR spectroscopy of human dementia. Neuroimaging Clin N Am 1998;8(4):809–822
22 Kantarci K. 1H magnetic resonance spectroscopy in dementia. Br J Radiol 2007;80(Spec No 2):S146–S152
23 Firbank MJ, Harrison RM, O'Brien JT. A comprehensive review of proton magnetic resonance spectroscopy studies in dementia and Parkinson's disease. Dement Geriatr Cogn Disord 2002; 14(2):64–76
24 Grover VP, Dresner MA, Forton DM, et al. Current and future applications of magnetic resonance imaging and spectroscopy of the brain in hepatic encephalopathy. World J Gastroenterol 2006;12(19):2969–2978
25 Ross BD, Danielsen ER, Blüml S. Proton magnetic resonance spectroscopy: the new gold standard for diagnosis of clinical and subclinical hepatic encephalopathy? Dig Dis 1996; 14(Suppl 1):30–39
26 Cecil KM. MR spectroscopy of metabolic disorders. Neuroimaging Clin N Am 2006;16(1):87–116, viii viii
27 Moffett JR, Ross B, Arun P, Madhavarao CN, Namboodiri AM. N-Acetylaspartate in the CNS: from neurodiagnostics to neurobiology. Prog Neurobiol 2007;81(2):89–131
28 Saneto RP, Friedman SD, Shaw DW. Neuroimaging of mitochondrial disease. Mitochondrion 2008;8(5–6):396–413
29 Schiffmann R, van der Knaap MS. The latest on leukodystrophies. Curr Opin Neurol 2004;17(2):187–192
30 Cady EB. Magnetic resonance spectroscopy in neonatal hypoxic-ischaemic insults. Childs Nerv Syst 2001;17(3):145–149
31 Saunders DE. MR spectroscopy in stroke. Br Med Bull 2000; 56(2):334–345
32 Ricci PE Jr. Proton MR spectroscopy in ischemic stroke and other vascular disorders. Neuroimaging Clin N Am 1998;8(4):881–900
33 De Stefano N, Filippi M. MR spectroscopy in multiple sclerosis. J Neuroimaging 2007;17(Suppl 1):31S–35S
34 Narayana PA. Magnetic resonance spectroscopy in the monitoring of multiple sclerosis. J Neuroimaging 2005;15(4, Suppl):46S–57S
35 Arnold DL, De Stefano N, Narayanan S, Matthews PM. Proton MR spectroscopy in multiple sclerosis. Neuroimaging Clin N Am 2000;10(4):789–798, ix–x
36 Lin AP, Liao HJ, Merugumala SK, Prabhu SP, Meehan WP III, Ross BD. Metabolic imaging of mild traumatic brain injury. Brain Imaging Behav 2012;6(2):208–223
37 Marino S, Ciurleo R, Bramanti P, Federico A, De Stefano N. 1H-MR spectroscopy in traumatic brain injury. Neurocrit Care 2011; 14(1):127–133
38 Garnett MR, Cadoux-Hudson TA, Styles P. How useful is magnetic resonance imaging in predicting severity and outcome in traumatic brain injury? Curr Opin Neurol 2001;14(6):753–757
39 Brooks WM, Friedman SD, Gasparovic C. Magnetic resonance spectroscopy in traumatic brain injury. J Head Trauma Rehabil 2001;16(2):149–164
40 Panigrahy A, Blüml S. Advances in magnetic resonance imaging of the injured neonatal brain. Pediatr Ann 2008;37(6):395–402
41 Panigrahy A, Borzage M, Blüml S. Basic principles and concepts underlying recent advances in magnetic resonance imaging of the developing brain. Semin Perinatol 2010;34(1):3–19
42 Hoon AH Jr, Melhem ER. Neuroimaging: applications in disorders of early brain development. J Dev Behav Pediatr 2000;21(4): 291–302
43 Kułak W, Sobaniec W. Molecular mechanisms of brain plasticity: neurophysiologic and neuroimaging studies in the developing patients. Rocz Akad Med Bialymst 2004;49:227–236
44 Martin WRW. MR spectroscopy in neurodegenerative disease. Mol Imaging Biol 2007;9(4):196–203
45 Pioro EP. Proton magnetic resonance spectroscopy (1H-MRS) in ALS. Amyotroph Lateral Scler Other Motor Neuron Disord 2000;1 (Suppl 2):S7–S16
46 Harris RE, Clauw DJ. Imaging central neurochemical alterations in chronic pain with proton magnetic resonance spectroscopy. Neurosci Lett 2012;520(2):192–196
47 Mountford CE, Stanwell P, Lin A, Ramadan S, Ross B. Neurospectroscopy: the past, present and future. Chem Rev 2010;110 (5):3060–3086
48 Broniscer A, Gajjar A, Bhargava R, et al. Brain stem involvement in children with neurofibromatosis type 1: role of magnetic resonance imaging and spectroscopy in the distinction from diffuse pontine glioma. Neurosurgery 1997;40(2):331–337, discussion 337–338
49 Castillo M, Kwock L, Courvoisie HE, Hooper SR, Greenwood RS. Proton MR spectroscopy in psychiatric and neurodevelopmental childhood disorders: early experience. Neuroimaging Clin N Am 1998;8(4):901–912
50 Lin DD, Barker PB. Neuroimaging of phakomatoses. Semin Pediatr Neurol 2006;13(1):48–62
51 Arora A, Neema M, Stankiewicz J, et al. Neuroimaging of toxic and metabolic disorders. Semin Neurol 2008;28(4):495–510
52 Licata SC, Renshaw PF. Neurochemistry of drug action: insights from proton magnetic resonance spectroscopic imaging and their relevance to addiction. Ann N Y Acad Sci 2010;1187:148–171
53 Meyerhoff DJ, Durazzo TC. Proton magnetic resonance spectroscopy in alcohol use disorders: a potential new endophenotype? Alcohol Clin Exp Res 2008;32(7):1146–1158
54 Panigrahy A, Blüml S. Advances in magnetic resonance neuroimaging techniques in the evaluation of neonatal encephalopathy. Top Magn Reson Imaging 2007;18(1):3–29
55 Hunter JV, Wang ZJ. MR spectroscopy in pediatric neuroradiology. Magn Reson Imaging Clin N Am 2001;9(1):165–189, ix ix
56 Nucci-da-Silva MP, Amaro E Jr. A systematic review of magnetic resonance imaging and spectroscopy in brain injury after drowning. Brain Inj 2009;23(9):707–714
57 Gómez-Ansón B, MacManus DG, Parker GJ, et al. In vivo 1H-magnetic resonance spectroscopy of the spinal cord in humans. Neuroradiology 2000;42(7):515–517
58 Lammertse D, Dungan D, Dreisbach J, et al; National Institute on Disability and Rehabilitation. Neuroimaging in traumatic spinal cord injury: an evidence-based review for clinical practice and research. J Spinal Cord Med 2007;30(3):205–214
59 Caverzasi E, Pichiecchio A, Calligaro A, et al. Complications in major depressive disorder therapy: a review of magnetic resonance spectroscopy studies. Funct Neurol 2008;23(3):129–132
60 Karl A, Werner A. The use of proton magnetic resonance spectroscopy in PTSD research—meta-analyses of findings and methodological review. Neurosci Biobehav Rev 2010;34(1):7–22
61 Keshavan MS, Stanley JA, Pettegrew JW. Magnetic resonance spectroscopy in schizophrenia: methodological issues and findings—part II. Biol Psychiatry 2000;48(5):369–380
62 Stanley JA, Pettegrew JW, Keshavan MS. Magnetic resonance spectroscopy in schizophrenia: methodological issues and findings—part I. Biol Psychiatry 2000;48(5):357–368
63 Sundgren PC. MR spectroscopy in radiation injury. AJNR Am J Neuroradiol 2009;30(8):1469–1476
64 Nelson SJ. Imaging of brain tumors after therapy. Neuroimaging Clin N Am 1999;9(4):801–819
65 Payne GS, Leach MO. Applications of magnetic resonance spectroscopy in radiotherapy treatment planning. Br J Radiol 2006;79 (Spec No 1):S16–S26

66 Lai PH, Hsu SS, Lo YK, Ding SW. Role of diffusion-weighted imaging and proton MR spectroscopy in distinguishing between pyogenic brain abscess and necrotic brain tumor. Acta Neurol Taiwan 2004;13(3):107–113
67 Peterson PL, Axford JS, Isenberg D. Imaging in CNS lupus. Best Pract Res Clin Rheumatol 2005;19(5):727–739
68 Tanabe J, Weiner MW. MRI-MRS of the brain in systemic lupus erythematosus. How do we use it to understand causes of clinical signs? Ann N Y Acad Sci 1997;823:169–184
69 Caverzasi E, Pichiecchio A, Poloni GU, et al. Magnetic resonance spectroscopy in the evaluation of treatment efficacy in unipolar major depressive disorder: a review of the literature. Funct Neurol 2012;27(1):13–22
70 Gonzalez-Toledo E, Kelley RE, Minagar A. Role of magnetic resonance spectroscopy in diagnosis and management of multiple sclerosis. Neurol Res 2006;28(3):280–283
71 Lin A, Ross BD, Harris K, Wong W. Efficacy of proton magnetic resonance spectroscopy in neurological diagnosis and neurotherapeutic decision making. NeuroRx 2005;2(2):197–214
72 Moats RA, Watson L, Shonk T, et al. Added value of automated clinical proton MR spectroscopy of the brain. J Comput Assist Tomogr 1995;19(3):480–491
73 Webb PG, Sailasuta N, Kohler SJ, Raidy T, Moats RA, Hurd RE. Automated single-voxel proton MRS: technical development and multisite verification. Magn Reson Med 1994;31(4):365–373
74 ACR–ASNR Practice Guideline for the Performance and Interpretation of Magnetic Resonance Spectroscopy of the Central Nervous System. 2008. Available at: http://www.acr.org/~/media/B0AF516E53234DA399EF305525504249.pdf. Accessed October 10, 2012
75 Rosen Y, Lenkinski RE. Recent advances in magnetic resonance neurospectroscopy. Neurotherapeutics 2007;4(3):330–345
76 Ashwal S, Holshouser BA, Shu SK, et al. Predictive value of proton magnetic resonance spectroscopy in pediatric closed head injury. Pediatr Neurol 2000;23(2):114–125
77 Camicioli RM, Korzan JR, Foster SL, et al. Posterior cingulate metabolic changes occur in Parkinson's disease patients without dementia. Neurosci Lett 2004;354(3):177–180
78 Gropman A. Brain imaging in urea cycle disorders. Mol Genet Metab 2010;100(Suppl 1):S20–S30
79 Shimizu E, Hashimoto K, Ochi S, et al. Posterior cingulate gyrus metabolic changes in chronic schizophrenia with generalized cognitive deficits. J Psychiatr Res 2007;41(1–2):49–56
80 Hsu YY, Chen MC, Lim KE, Chang C. Reproducibility of hippocampal single-voxel proton MR spectroscopy and chemical shift imaging. AJR Am J Roentgenol 2001;176(2):529–536
81 Kreis R. Issues of spectral quality in clinical 1H-magnetic resonance spectroscopy and a gallery of artifacts. NMR Biomed 2004;17(6):361–381
82 Kallenberg K, Bock HC, Helms G, et al. Untreated glioblastoma multiforme: increased myo-inositol and glutamine levels in the contralateral cerebral hemisphere at proton MR spectroscopy. Radiology 2009;253(3):805–812
83 Sundgren PC, Nagesh V, Elias A, et al. Metabolic alterations: a biomarker for radiation-induced normal brain injury-an MR spectroscopy study. J Magn Reson Imaging 2009;29(2):291–297
84 Estève F, Rubin C, Grand S, Kolodié H, Le Bas JF. Transient metabolic changes observed with proton MR spectroscopy in normal human brain after radiation therapy. Int J Radiat Oncol Biol Phys 1998;40(2):279–286
85 Sijens PE, Oudkerk M, van Dijk P, Levendag PC, Vecht CJ. 1H MR spectroscopy monitoring of changes in choline peak area and line shape after Gd-contrast administration. Magn Reson Imaging 1998;16(10):1273–1280
86 Sijens PE, van den Bent MJ, Nowak PJ, van Dijk P, Oudkerk M. 1H chemical shift imaging reveals loss of brain tumor choline signal after administration of Gd-contrast. Magn Reson Med 1997;37(2):222–225
87 Smith JK, Kwock L, Castillo M. Effects of contrast material on single-volume proton MR spectroscopy. AJNR Am J Neuroradiol 2000;21(6):1084–1089
88 Lima EC, Otaduy MC, Tsunemi M, et al. The effect of paramagnetic contrast in choline peak in patients with glioblastoma multiforme might not be significant. AJNR Am J Neuroradiol 2012
89 Murphy PS, Dzik-Jurasz AS, Leach MO, Rowland IJ. The effect of Gd-DTPA on T(1)-weighted choline signal in human brain tumours. Magn Reson Imaging 2002;20(1):127–130
90 Lin AP, Ross BD. Short-echo time proton MR spectroscopy in the presence of gadolinium. J Comput Assist Tomogr 2001;25(5):705–712
91 Murphy PS, Leach MO, Rowland IJ. The effects of paramagnetic contrast agents on metabolite protons in aqueous solution. Phys Med Biol 2002;47(6):N53–N59
92 Candiota AP, Majós C, Julià-Sapé M, et al. Non-invasive grading of astrocytic tumours from the relative contents of myo-inositol and glycine measured by in vivo MRS. JBR-BTR 2011;94(6):319–329
93 Kim JH, Chang KH, Na DG, et al. 3T 1H-MR spectroscopy in grading of cerebral gliomas: comparison of short and intermediate echo time sequences. AJNR Am J Neuroradiol 2006;27(7):1412–1418
94 Galanaud D, Chinot O, Nicoli F, et al. Use of proton magnetic resonance spectroscopy of the brain to differentiate gliomatosis cerebri from low-grade glioma. J Neurosurg 2003;98(2):269–276
95 Panigrahy A, Krieger MD, Gonzalez-Gomez I, et al. Quantitative short echo time 1H-MR spectroscopy of untreated pediatric brain tumors: preoperative diagnosis and characterization. AJNR Am J Neuroradiol 2006;27(3):560–572
96 Inglese M, Spindler M, Babb JS, Sunenshine P, Law M, Gonen O. Field, coil, and echo-time influence on sensitivity and reproducibility of brain proton MR spectroscopy. AJNR Am J Neuroradiol 2006;27(3):684–688
97 Provencher SW. Estimation of metabolite concentrations from localized in vivo proton NMR spectra. Magn Reson Med 1993;30(6):672–679
98 Naressi A, Couturier C, Castang I, de Beer R, Graveron-Demilly D. Java-based graphical user interface for MRUI, a software package for quantitation of in vivo/medical magnetic resonance spectroscopy signals. Comput Biol Med 2001;31(4):269–286
99 Delikatny EJ, Chawla S, Leung DJ, Poptani H. MR-visible lipids and the tumor microenvironment. NMR Biomed 2011;24(6):592–611
100 Haseler LJ, Arcinue E, Danielsen ER, Bluml S, Ross BD. Evidence from proton magnetic resonance spectroscopy for a metabolic cascade of neuronal damage in shaken baby syndrome. Pediatrics 1997;99(1):4–14
101 Howe FA, Barton SJ, Cudlip SA, et al. Metabolic profiles of human brain tumors using quantitative in vivo 1H magnetic resonance spectroscopy. Magn Reson Med 2003;49(2):223–232
102 Harris K, Lin A, Bhattacharya P, Tran T, Wong W, Ross B. Regulation of NAA-synthesis in the human brain in vivo: Canavan's disease, Alzheimer's disease and schizophrenia. Adv Exp Med Biol 2006;576:263–273, discussion 361–363
103 Ross BD. Biochemical considerations in 1H spectroscopy. Glutamate and glutamine; myo-inositol and related metabolites. NMR Biomed 1991;4(2):59–63
104 Stöckler S, Holzbach U, Hanefeld F, et al. Creatine deficiency in the brain: a new, treatable inborn error of metabolism. Pediatr Res 1994;36(3):409–413
105 Glunde K, Bhujwalla ZM, Ronen SM. Choline metabolism in malignant transformation. Nat Rev Cancer 2011;11(12):835–848
106 Ross BD, Bluml S, Cowan R, Danielsen E, Farrow N, Gruetter R. In vivo magnetic resonance spectroscopy of human brain: the biophysical basis of dementia. Biophys Chem 1997;68(1–3):161–172
107 Pérez-Ruiz A, Julià-Sapé M, Mercadal G, Olier I, Majós C, Arús C. The INTERPRET decision-support system version 3.0 for evaluation of magnetic resonance spectroscopy data from human brain

tumours and other abnormal brain masses. BMC Bioinformatics 2010;11:581
108 Srinivasan R, Vigneron D, Sailasuta N, Hurd R, Nelson SJ. A comparative study of myo-inositol quantification using LCmodel at 1.5 T and 3.0 T with 3 D 1H proton spectroscopic imaging of the human brain. Magn Reson Imaging 2004;22(4):523–528
109 Cigna Medical Coverage Policy no.0244. 2010. Available at: http://www.cigna.com/customer_care/healthcare_professional/coverage_positions/medical/mm_0244_coveragepositioncriteria_magnetic_resonance_spectroscopy.pdf. Accessed October 1, 2012
110 Anthem Medical Policy RAD. 00022. 2012. Available at: http://www.anthem.com/medicalpolicies/policies/mp_pw_a053262.htm. Accessed October 1, 2012
111 Blue Cross Blue Shield of Delaware Medical Policy 6.01.34. 2012. Available at: http://www.bcbsde.com/ProviderPolicies/public_site/6.01.34_Magnetic_Resonance_Spectroscopy.htm. Accessed October 1, 2012
112 Blue Cross Blue Shield Blue Care Network Medical Policy Michigan 110111.MXD. 2011. . Available at: http://www.bcbsm.com/mprApp/MedicalPolicyDocument?fileId=2036662. Accessed October 1, 2012
113 Excellus Policy Number 6.01.03. 2011. Available at: http://www.excellusbcbs.com/wps/wcm/connect/90e97c8044fba9ed9be4fbef58edd5a7/mp+mrs+tac+11.pdf?MOD=AJPERES. Accessed October 1, 2012
114 Highmark West Virginia Medical Policy X-50. 2011. Available at: http://www.highmarkbcbswv.com/medpolicy/X-50-006.html. Accessed October 1, 2012
115 Lifewise Medical Policy 6.01.514. 2012. Available at: http://www.lifewisewa.com/lwwa/groups/public/documents/medicalpolicy/cmi_041957.htm. Accessed October 1, 2012
116 Medical Fee Schedule OWCP. 2010. Available at: http://www.dol.gov/owcp/regs/feeschedule/fee/fee10/PublicUseFileDirectory2010.htm. Accessed October 1, 2012
117 Lin A, Clements V, Tran T, Ross B. Reimbursement for Magnetic Resonance Spectroscopy. In: Proceedings 17th Scientific Meeting, International Society for Magnetic Resonance in Medicine. Berkeley, CA: International Society for Magnetic Resonance in Medicine; 2009:2509
118 Fryback DG, Thornbury JR. The efficacy of diagnostic imaging. Med Decis Making 1991;11(2):88–94